Title

Reductive Elimination from Phosphine-Ligated Alkylpalladium(II) Amido Complexes To Form sp3 Carbon-Nitrogen Bonds.

Journal

Journal of the American Chemical Society, 140(14)

Authors

Peacock, D
Jiang, Quan
Hanley, Patrick
et al.

Publication Date

2018-04-11

DOI

10.1021/jacs.8b00928

Peer reviewed

Published in final edited form as:

J Am Chem Soc. 2018 April 11; 140(14): 4893–4904. doi:10.1021/jacs.8b00928.

Reductive Elimination from Phosphine-Ligated Alkylpalladium(II) Amido Complexes To Form sp^3 Carbon–Nitrogen Bonds

D. Matthew Peacock[†], **Quan Jiang**[‡], **Patrick S. Hanley**[†,§], **Thomas R. Cundari**[*,‡], **John F. Hartwig**[*,†]

[†]Department of Chemistry, University of California, Berkeley, California 94720, United States

[‡]Department of Chemistry and Center for Advanced Scientific Computing and Modeling, University of North Texas, Denton, Texas 76203, United States

Abstract

We report the formation of phosphine-ligated alkylpalladium(II) amido complexes that undergo reductive elimination to form alkyl-nitrogen bonds and a combined experimental and computational investigation of the factors controlling the rates of these reactions. The free-energy barriers to reductive elimination from *t*-Bu_3P-ligated complexes were significantly lower (ca. 3 kcal/mol) than those previously reported from NHC-ligated complexes. The rates of reactions from complexes containing a series of electronically and sterically varied anilido ligands showed that the reductive elimination is slower from complexes of less electron-rich or more sterically hindered anilido ligands than from those containing more electron-rich and less hindered anilido ligands. Reductive elimination of alkylamines also occurred from complexes bearing bidentate P,O ligands. The rates of reactions of these four-coordinate complexes were slower than those for reactions of the three-coordinate, *t*-Bu_3P-ligated complexes. The calculated pathway for reductive elimination from rigid, 2-methoxyarylphosphine-ligated complexes does not involve initial dissociation of the oxygen. Instead, reductive elimination is calculated to occur directly from the four-coordinate complex in concert with a lengthening of the Pd–O bond. To investigate this effect experimentally, a four-coordinate Pd(II) anilido complex containing a flexible, aliphatic linker between the P and O atoms was synthesized. Reductive elimination from this complex was faster than that from the analogous complex containing the more rigid, aryl linker. The flexible linker enables full dissociation of the ether ligand during reductive elimination, leading to the faster reaction of this complex.

Graphical Abstract

[*]**Corresponding Authors:** jhartwig@berkeley.edu, t@unt.edu.

[§]Core Research & Development, The Dow Chemical Company, 1776 Building, Midland, Michigan 48674, United States.

Supporting Information

The Supporting Information is available free of charge on the ACS Publications website at DOI: 10.1021/jacs.8b00928.

Experimental details, NMR spectra, crystallographic data, computational details, and optimized coordinates (PDF)

Crystallographic data for **8a** (CIF)

Crystallographic data for **8b** (CIF)

Crystallographic data for **8e** (CIF)

The authors declare no competing financial interest.

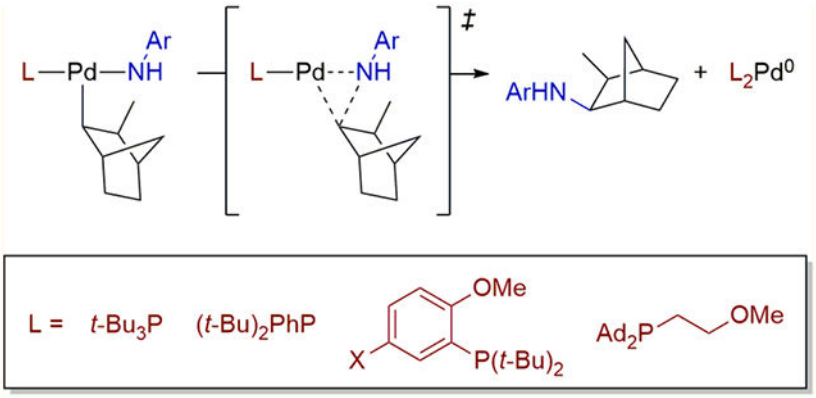

INTRODUCTION

Reductive eliminations to form carbon–nitrogen bonds are important steps in many reactions that produce amines catalyzed by or mediated by transition-metal complexes. Reactions to form sp^2 carbon–nitrogen bonds from aryl- and heteroarylpalladium(II) complexes have been well studied.[1,2] However, reductive eliminations to form the analogous sp^3 C–N bonds in alkylamines from alkylmetal amido complexes are rare, and the factors controlling the rates and scope of this elementary reaction are poorly defined. An increased understanding of this fundamental organometallic reaction could enable the development of new methods to construct sp^3 C–N bonds by catalytic reactions, such as C–H bond functionalization, olefin functionalization, or nucleophilic substitution.

Complexes of palladium(IV)[3–5] and other high-valent metal centers[6–9] have been reported to undergo reductive elimination to form sp^3 C–N bonds. However, examples of such reductive eliminations from low-valent metal complexes are more limited. Our group reported the first reductive eliminations from alkylpalladium(II) amido complexes (Scheme 1), in part motivated by reports of catalytic reactions that could occur through these intermediates.[10–12] Benzylpalladium(II) and alkylpalladium(II) complexes have been shown to react by two distinct mechanisms. Four-coordinate, bisphosphine-ligated benzylpalladium(II) amido complexes undergo reductive elimination by a stepwise mechanism involving initial dissociation of an anionic amido ligand, followed by nucleophilic attack of this anion on the coordinated benzyl ligand.[13] This pathway results in inversion of configuration at the palladium-bound carbon atom. In contrast, three-coordinate, *N*-heterocyclic carbene (NHC)-ligated palladium(II) complexes bearing the unstabilized alkyl ligand *syn*-3-methylnorborn-2-yl underwent reductive elimination by a concerted pathway, resulting in retention of configuration at the palladium-bound carbon atom.[14]

The reported examples of reductive elimination from NHC-ligated (*syn*-3-methylnorborn-2-yl)palladium(II) complexes occurred with high kinetic barriers (≥26 kcal/mol at 90 °C). Therefore, we have sought to understand the properties of the complexes and ligands that control the rates of reaction and to identify complexes that undergo reductive elimination more rapidly. We have also sought to determine whether the rates of concerted reductive elimination to form sp^3 C–N bonds follow the trends previously reported for concerted

reductive eliminations from d^8 transition metal centers that form sp^2–sp^3 C–C, sp^3–sp^3 C–C, and sp^2 C–N bonds.

Herein, we report the preparation of a series of phosphine-ligated palladium(II) amido complexes that undergo reductive elimination to form alkyl–nitrogen bonds. These studies reveal, by both experimental and computational methods, the effects controlling the structures of the Pd(II) anilido intermediates and the barriers to reductive elimination from these complexes. These results led to the discovery that the reductive elimination to form alkylamines from four-coordinate complexes containing particular P,O ligands is fast and depends on the ability of the Pd–O bond to lengthen or dissociate during reductive elimination.

RESULTS AND DISCUSSION

Alkylpalladium(II) Amido Complexes Ligated by Monophosphines.

Palladium(II) complexes ligated by bulky monophosphines, such as tri-*tert*-butylphosphine (*t*-Bu_3P), undergo reductive elimination reactions that are slow or do not occur at all from analogous complexes containing less sterically demanding ligands.[2,15,16] Therefore, we investigated the potential of alkylpalladium complexes ligated by bulky monophosphines to undergo reductive elimination to form the sp^3 carbon–nitrogen bond in alkylamines.

Synthesis and Reactions of t-Bu_3P-ligated Complexes.—The preparation of *t*-Bu_3P-ligated alkylpalladium(II) anilido complexes was conducted in two steps from a known complex by the sequence shown in Scheme 2. Treatment of the olefin-ligated precursor 1,5-cyclooctadiene (*syn*-3-methylnorborn-2-yl)palladium(II) chloride with *t*-Bu_3P at ambient temperature in THF generated the three-coordinate complex (*t*-Bu_3P)Pd(3-CH_3norborn-2-yl)Cl (**1**). This complex was stable at ambient temperature and crystallized as red blocks in 81% yield. The reaction of complex **1** with sodium *tert*-butoxide (NaO*t*-Bu), *t*-Bu_3P, and a series of arylamines at ambient temperature formed Pd(II) anilido complexes **2a**–**i** in 76–92% yield with (*t*-$Bu_3P)_2Pd^0$ as a minor side product, as determined by ^{31}P NMR spectroscopy. Although *t*-Bu_3P is not consumed by the reaction, complexes bearing unhindered anilido ligands formed in lower yields when the reaction was performed without added *t*-Bu_3P.

The *t*-Bu_3P-ligated Pd(II) anilido complexes were typically unstable at ambient temperature and highly soluble in organic solvents, preventing recrystallization and isolation in pure form. However, the molecular weights (*M*) of **2g** and **2i** were approximated by ^{19}F NMR diffusion ordered spectroscopy (DOSY) experiments, and these molecular weight values agreed well with the expected values for monomeric, three-coordinate alkylpalladium(II) amido complexes (Table 1, entries 1 and 2). Furthermore, ^1H NMR nuclear Overhauser effect spectra (NOESY) of **2i** were consistent with a three-coordinate T-shaped or distorted T-shaped structure. Specifically, correlations were observed between the *endo* hydrogen on the palladium-bound carbon and the *tert*-butyl groups on the phosphine, as well as between the *exo* methyl group on the alkyl ligand and the NH proton of the anilido ligand (see Supporting Information (SI) for spectra and assignments).

Reductive Elimination from Alkylpalladium(II) Amido Complexes Ligated by t-Bu_3P.—Due to the instability of *t*-Bu_3P-ligated Pd(II) anilido complexes at room temperature, studies of the reductive elimination to form alkylamines were conducted with complexes prepared *in situ*. Complexes **2a**–**i** underwent reductive elimination at 40–65 °C to form the corresponding norbornylamines **3a**–**i** in yields of 59% or higher (Scheme 2). Excess *t*-Bu_3P (included during the formation of **2a**–**i**) served to trap the palladium-containing product as (*t*-$Bu_3P)_2Pd^0$.

The reductive-elimination reactions were monitored by ^1H or ^{19}F NMR spectroscopy at 40–65 °C in THF-d_8 or THF. All reactions of *t*-Bu_3P-ligated Pd(II) anilido complexes occurred with a first-order decay. The rate constants for reductive elimination (k_{RE}) and the corresponding free energies of activation ($\Delta G^{\ddagger}$) are shown in Table 2.

The kinetic data for reductive elimination from complexes bearing *meta*- and *para*-substituted anilido ligands (entries 1–7) were analyzed with a Hammett plot. A reasonable correlation ($R^2 = 0.95$) between Log k_X/k_H and σ was observed with a ρ value of −2.0 (Figure 1). This result suggests that complexes with less stabilization of a partial negative charge on nitrogen react faster than those with more stabilization of the charge, and the magnitude of ρ suggests that significant negative charge accumulates on nitrogen. The *ortho*-*tert*-butyl-substituted **2h** underwent reductive elimination with the highest kinetic barrier of any *t*-Bu_3P-ligated complex that was investigated. Thus, reductive elimination generally occurred fastest from complexes bearing unhindered, electron-rich anilido ligands. Further studies were conducted primarily with 4-fluoro-2-methoxyaniline because the barrier for reductive elimination from the *ortho*-methoxy substituted **2i** was similar to that for reductive elimination from the unsubstituted **2a**, but the reaction of **2i** could be followed by ^{19}F NMR spectroscopy and occurred in high yield.

We sought to determine whether reductive elimination occurs directly from the three-coordinate complex observed in solution or from a different intermediate after association or dissociation of a ligand. The reaction of the *ortho*-methoxy substituted **2i** to form **3i** was determined to be zeroth-order in *t*-Bu_3P, and the yield of **3i** did not vary significantly with the concentration of *t*-Bu_3P (Figure 2a). These results suggest that the mechanism of reductive elimination does not involve either association or reversible dissociation of *t*-Bu_3P prior to the transition state.

Further insight into the mechanism of reductive elimination was obtained by measuring the enthalpy and entropy of activation. An Eyring analysis (40–60 °C) of the reductive elimination from **2i** provided the parameters $\Delta H^{\ddagger} = 19 \pm 1$ kcal/mol and a $\Delta S^{\ddagger} = -14 \pm 4$ eu (Figure 2b). The negative value of $\Delta S^{\ddagger}$ is inconsistent with a pathway involving ligand dissociation prior to reductive elimination. The magnitude of $\Delta S^{\ddagger}$ is consistent with either an associative process or a unimolecular process in which the transition state is more ordered than the ground state. Because the zeroth-order dependence on [*t*-Bu_3P] rules out an associative pathway, these results support a mechanism for reductive elimination occurring directly from the three-coordinate complex observed in solution.

Synthesis of Alkylpalladium(II) Complexes Ligated by t-Bu_2PhP.—To dissect the steric and electronic effects on the reductive elimination to form the alkyl-nitrogen bond from phosphine-ligated palladium(II), we studied complexes containing di-*tert*-butylarylphosphines. Complexes of such ligands would enable the steric and electronic properties to be varied by substitution on the aryl group.

The preparation of a *t*-Bu_2PhP-ligated alkylpalladium(II) anilido complex was attempted by the same two-step sequence described for the synthesis of complexes **2a**–**i**. Treatment of cyclooctadiene-ligated (*syn*-3-methylnorborn-2-yl)palladium(II) chloride with *t*-Bu_2PhP at ambient temperature in THF generated (*t*-Bu_2PhP)Pd(3-CH_3norborn-2-yl)Cl (**4a**), which was isolated as an off-white powder in 64% yield after recrystallization. Complex **4a** reacted with 4-fluoro-2-methox-yaniline and NaO*t*-Bu at ambient temperature with 3 equiv of *t*-Bu_2PhP in THF to produce a complicated mixture of palladium complexes (Scheme 3). The species that formed in highest concentration in this mixture (as determined by ^{19}F or ^{31}P NMR spectroscopy) was assigned to be the bimetallic complex **6a**, which formed in approximately 29% yield (based on 2:1 stoichiometry of **4a** to **6a**). Complex **6a** formed in a higher yield of 63% when the same reaction was performed with LiHMDS as a base in toluene.

The identity of bimetallic amido complex **6a** was deduced by NMR spectroscopy using samples prepared *in situ* by the reaction of chloride complex **4a**, 4-fluoro-2-methoxyaniline, and LiHMDS in toluene.[17] Complex **6a** contains one phosphine ligand, two inequivalent alkyl ligands, and two inequivalent anilido ligands. The formation of approximately 1 equiv of free *t*-Bu_2PhP per product was also observed, which accounts for the 1:2 ratio of phosphine to palladium in **6a**. Furthermore, the molecular weight of the complex, as determined by ^{19}F NMR DOSY experiments, was approximately 943 (Table 1, entry 3). These results are consistent with the assignment of **6a** as a bimetallic complex lacking one of the starting phosphine ligands (expected M = 934). ^{1}H NMR NOESY and ^{1}H–^{31}P HMBC experiments suggested that the two palladium centers are linked by a single bridging anilido ligand (see the SI for spectra and partial assignments). These experiments are consistent with the structure drawn in Scheme 3.

The observation of a monometallic complex with *t*-Bu_3P as a ligand but a bimetallic complex with *t*-Bu_2PhP as a ligand shows that increasing steric bulk at phosphorus leads to a decrease in relative concentration of the bimetallic complex. The greater electron donation by *t*-Bu_3P than by *t*-Bu_2PhP also would be expected to favor the monometallic complex over the bimetallic complex. However, a mixture of Pd(II) anilido complexes was observed to form from reactions of (*t*-Bu_2CyP)Pd(3-CH_3norborn-2-yl)Cl (**4b**), 4-fluoro-2-methoxyaniline, and a base (see the SI for details). The electron-donating properties of *t*-Bu_3P and *t*-Bu_2CyP are similar.[18,19] Therefore, these results suggest that the steric properties of the ancillary ligand, not the electronic properties, primarily determine whether monometallic or bimetallic structures are favored.

Reductive Elimination from Bimetallic Alkylpalladium(II) Amido Complex 6a.—Heating of the mixture of complexes described in Scheme 3 at 65 °C in THF for 3 h formed the norbornylamine product **3i** in 75% yield (based on **4a**) (Scheme 4). Under these

conditions, the remainder of the mass balance (with respect to the amine) was 4-fluoro-2-methoxyaniline, as determined by ^{19}F NMR spectroscopy. The yield of **3i** greatly exceeds the yield of any of the individual palladium complexes in the solution, indicating that multiple species undergo reductive elimination or that multiple species equilibrate prior to reductive elimination.

To gain insight into the mechanism of reductive elimination from the *t*-Bu$_2$PhP-ligated bimetallic complex **6a**, the order in phosphine was measured. The initial rate (*r*) of formation of **3i** was measured for reactions conducted with 1, 4, or 9 equiv of added *t*-Bu$_2$PhP (Figure 3, Table S-6, and Figure S-5). In contrast to the rate of reaction with *t*-Bu$_3$P, the rate of the reaction with *t*-Bu$_2$PhP was dependent on the concentration of phosphine. The approximately half-order dependence is consistent with a mechanism in which **6a** (or other bimetallic species lacking a phosphine ligand) undergoes fast reversible association of one *t*-Bu$_2$PhP to form 2 equiv of the monometallic intermediate prior to reductive elimination (Scheme 4). Due to its analogy with the *t*-Bu$_3$P-ligated complex **2i**, we proposed that complex **5a** is likely the intermediate that undergoes reductive elimination of the amine.

Synthesis and Reactivity of Four-Coordinate Alkylpalladium(II) Amido Complexes Bearing 2-Methoxyarylphosphines.

Because reductive elimination from the *t*-Bu$_2$PhP-ligated complexes is a multistep process involving multiple (likely equilibrating) Pd(II) anilido complexes, this system was not amenable to dissecting the effects of ancillary ligands on the rate of reductive elimination. Therefore, we sought to identify a class of complexes that was monometallic and contained a phosphine that could possess varied steric and electronic properties. It was found that the formation of bimetallic species and the dissociation of the di-*tert*-butyl arylphosphine ligand could be prevented by introducing a second coordinating group at the *ortho*-position of the arylphosphine.

Synthesis of Alkylpalladium(II) Complexes Ligated by 2-Methoxyarylphosphines.—

The [R$_2$(2-(OMe)Ar)P]Pd(3-CH$_3$norborn-2-yl)Cl complexes **7a**–**d** bearing 2-methoxyaryl groups on phosphorus were prepared from the reactions of (COD)Pd(3-CH$_3$norborn-2-yl)Cl and the corresponding phosphines in THF or DCM (Scheme 5). All four complexes formed as single isomers, with the phosphine *cis* to the alkyl ligand and the ether oxygen *cis* to the chloride. This geometry was established by NOESY correlations between the alkyl ligand and the *tert*-butyl or adamantyl groups on phosphorus.

A comparison of the ^{13}C NMR spectra of these complexes to those of the three-coordinate Pd(II) chloride complexes revealed a pronounced upfield shift of the resonance corresponding to the palladium-bound carbon of the alkyl ligand: 40.8 to 44.3 ppm for the four-coordinate complexes **7a**–**d** versus 57.9 to 64.2 ppm for the three-coordinate complexes **1** and **4a**–**b**. This difference in chemical shift suggests that coordination of the ether to palladium causes a significant increase in electron density at the alkyl ligand.

The reactions of the Pd(II) chloride complexes **7a**–**d** with 4-fluoro-2-methoxyaniline and LiHMDS with excess phosphine at ambient temperature in toluene generated the corresponding Pd(II) anilido complexes **8a**–**d** in yields of 85–89% by NMR spectroscopy

(Scheme 7). These four-coordinate complexes were moderately stable at ambient temperature, and samples suitable for analysis by X-ray diffraction were obtained from crystallization of **8a** and **8b** (Figure 4).

The ^{1}H NMR signals corresponding to the alkyl ligand in complex **8a** containing di-*tert*-butyl(*o*-anisyl)phosphine were assigned by two-dimensional NMR spectroscopy. An analysis of the ^{1}H NOESY correlations indicated that the alkyl ligand is positioned such that the *endo* face is close to the phosphine ligand, and the *exo* face is close to the anilido ligand. These results are consistent with the distorted square planar, solid-state structure obtained by X-ray diffraction. Therefore, any variation between the solid- and solution-state structures of this complex is small. Similar correlations were observed in the NOESY spectrum of the analogous three-coordinate, *t*-Bu_3P-ligated complex **2i**. This similarity suggests that the geometry at the metal and orientation of the ligands in **8a** are similar to those in **2i** (see the SI for spectra and assignments). Furthermore, ^{19}F NMR DOSY experiments with complex **8c** (which contains a second fluorine label on the ancillary ligand) confirmed that this complex, and presumably the other P,O-ligated complexes, is monometallic in solution (Table 1, entry4).

Reductive Elimination from Four-Coordinate Alkylpalladium(II) Amido Complexes Containing Rigid P,O Ligands.—Complexes **8a**–**d** bearing 2-methoxyarylphosphine ligands on palladium underwent reductive elimination of norbornylamine **3i** in yields of 52–83% after 14 or 48 h at 65 °C with 2 equiv of added phosphine to trap the Pd(0) product (Scheme 7). The yields of these reactions depended on the substituents on the phosphine ligand; the highest yield of 83% was obtained from the reaction of complex **8d** containing a 5-CF_3-subsituent on the phosphine aryl group.

The reductive eliminations from four-coordinate complexes **8a**–**d** were 12 to 120 times slower than that from the analogous three-coordinate, *t*-Bu_3P-ligated complex **2i** (Table 3). Previous studies on concerted reductive elimination reactions from d^8 transition metal centers have led to the conclusion that the rates of reductive elimination from four-coordinate, square planar complexes are typically slower than those from analogous three- or five-coordinate complexes.[20,21] Our observation that alkylpalladium amido complexes containing P,O ligands undergo reductive elimination more slowly than *t*-Bu_3P-ligated complexes is consistent with this general trend deduced from other classes of reductive eliminations. However, reductive elimination still occurs in moderate to good yield under mild conditions because the ether oxygen atom is a weak electron donor (*vide infra*).

Small changes to the steric properties of the complexes did not significantly influence the rate of reductive elimination. The rate of reaction of the di-*tert*-butyl(*o*-anisyl)phosphine-ligated complex **8a** was similar to that of the diadamantyl(*o*-anisyl)phosphine-ligated complex **8b** (Table 3, entries 2 and 3), and the solid-state structures of these two complexes (Figure 4) were similar to each other, as expected. Attempts to synthesize and investigate the reactivity of complexes bearing less sterically demanding P,O ligands were unsuccessful (see the SI for details).

The effects of the electronic properties of the phosphine on the rate of reductive elimination were more readily accessed and were significant. Reductive eliminations from complex **8c** containing the less electron-donating 5-F-substitued phosphine and from complex **8d** containing the less electron-donating 5-CF_3-substituted phosphine were 7 and 6 times faster, respectively, than that from **8a** (Table 3, entries 2 and 4). These results suggest that reductive elimination of alkylamines occurs faster from complexes bearing less electron-donating ancillary ligands than from complexes bearing more electron-donating ancillary ligands. This result is similar to that observed previously for other classes of reductive eliminations from palladium(II) complexes[22] and is consistent with our observation that *t*-Bu_3P-ligated complexes are much more reactive than the previously reported complexes containing more electron-donating[23,24] NHC ligands.

A Four-Coordinate Alkylpalladium(II) Complex Containing a More Flexible P,O Ligand.

Computational studies on the mechanism of reductive elimination from complexes **8a**–**d** containing rigid 2-methoxyarylphosphine ligands suggested that the variation in the length of the Pd–O bond in the ground state and in the transition state would impact the rate of reaction (*vide infra)*. To analyze this proposal experimentally, we prepared complexes containing a more flexible linker between the phosphorus and oxygen donors.

Synthesis of an Alkylpalladium(II) Complex Containing a Flexible Linker.—

The Pd(II) chloride precursor (Ad_2PCH_2-CH_2OCH_3-κ^2*P,O*)Pd(3-CH_3norborn-2-yl)Cl **7e** bearing a chelating 2-methoxyethyl group on phosphorus was prepared by the same method as described previously for the preparation of complexes **7a**–**d** (Scheme 6). After recrystallization, the sample contained a single isomer in which the phosphine and alkyl ligands are mutually *cis*, as determined by NMR spectroscopy. The aliphatic linker in this methoxyethylphosphine is more flexible than the aryl linker in the 2-methoxyarylphosphines. The aliphatic ether unit in **7e** is also expected to be a stronger electron donor than the aryl ether units in **7a**–**d**. This assertion is consistent with the higher-field ^{13}C NMR chemical shift of the palladium-bound alkyl carbon in **7e** than that of the palladium-bound alkyl carbon in **7a**–**d** (36.2 ppm for **7e** versus 40.8–44.3 ppm for **7a**–**d**).

The reaction of the 2-methoxyethylphosphine-ligated **7e** with 4-fluoro-2-methoxyaniline and LiHMDS in toluene produced the corresponding Pd(II) anilido complex **8e** in 90% yield by NMR spectroscopy (Scheme 6). Complex **8e** was isolated in a lower yield of 49% from a similar reaction of **7e** with lithium (4-fluoro-2-methoxyphenyl)amide in DCM. The flexibility of the linker between P and O creates the possibility that isomeric, κP structures could exist in equilibrium with **8e** (*vide infra*). However, an analysis of the correlations in the 2-D ^1H NOE spectrum indicates that a four-coordinate, $\kappa^2 P,O$ structure such as **8e** is the dominant species in solution (see the SI). Specifically, correlations were observed between the methoxy group of the ancillary ligand and the *ortho* H of the anilido ligand.

A crystal of **8e** suitable for X-ray diffraction was obtained. The solid-state structure of **8e** was similar to those of **8a** and **8b** (Figure 5). The Pd–O bond length in **8e** was 2.297 Å, which is only slightly longer than the 2.288 and 2.283 Å Pd–O bond lengths in **8a** and **8b**, respectively. Each of the other bond distances to palladium varied by less than 0.04 Å

between the three complexes, and the bond angles around palladium varied by less than 5°. These results suggest that the steric properties of the ligand in **8e** are similar to those of the ligands in **8a**–**d**.

Effect of the Flexibility of the Ligand Backbone on the Rate of Reductive Elimination.—Reductive elimination from complex **8e** containing the alkyl backbone was faster than that from complexes **8a**–**b** containing the more rigid aryl backbone. Complex **8e** underwent reductive elimination in the presence of 2 equiv of ligand at 65 °C in toluene to form norbornylamine **3i** in 92% yield. This yield was higher than those from the reactions of any of the 2-methoxyarylphosphine-ligated complexes (**8a**–**d**). The rate constant for reductive elimination from **8e** was 6 times larger than that for reductive elimination from **8b**, corresponding to a 1.2 kcal/mol lower barrier (Table 3, entry 4). We propose that this difference in reactivity is predominately due to the difference in flexibility between the aliphatic and aryl linkers, and this proposal was corroborated by computations (*vide infra*).

Effect of Chelating Group.—To investigate how the electron-donating property of the chelating group influences the rate of reductive elimination, we prepared [Ad_2PCH_2(2-C_5H_4N)-κ^2*P,N*]Pd(3-CH_3norborn-2-yl)NHAr **8f** containing a picolinyl group on phosphorus by the methods previously described (Scheme 7). The 1H NMR chemical shifts and NOE correlations observed for this complex are consistent with the four-coordinate structure drawn. Complex **8f** underwent unproductive decomposition at 65 °C in either THF or toluene, with no detectable formation of norbornylamine **3i**. This result implies that the barrier to reductive elimination from a complex containing a strongly electron-donating fourth ligand (such as a pyridine) located *trans* to the alkyl ligand is significantly higher than that from a complex containing a weak donor (such as an ether).[25]

Computational Studies.

Methods.—Computational studies were performed to investigate the effects of ancillary ligands on reductive elimination from palladium(II) amido complexes. Density functional theory calculations were conducted using Gaussian09[26] with the hybrid exchange functional B3LYP.[27] The Pd atom was represented by the Stevens/Basch/Krauss effective core potential and associated triple-ζ valence basis set.[28–30] The remaining main group atoms were represented by the 6–31+G(d) and 6–311++G(d,p) basis set for geometry optimizations in the gas phase and single-point calculations, respectively. Solvent effects (THF, ε = 7.4257) utilized the SMD[31] continuum model via single-point calculations on geometries optimized in the gas phase. Calculations of the free energies of activation for reductive elimination from palladium(II) amido complexes ligated by bulky *N*-heterocyclic carbene (NHC) ligands at the same level of theory matched the value measured experimentally.[14] The ground states were determined to be minima on their potential energy surfaces by the absence of imaginary frequencies, while the transition states were determined to be saddle points by the presence of a single imaginary frequency.

Computational Results. 1. Mechanism of Reductive Elimination from Four-Coordinate Complexes.—Reactions of the Pd(II) anilido complexes **8a**–**e** containing P,O ligands were investigated computationally to understand how the structure of the bidentate

ancillary ligands affects the rate of reductive elimination. The computed ground state geometries were similar to those measured by X-ray diffraction (Figures 4, 5, and 6). The computed free energy barrier for reductive elimination from **8a** was identical to that from the experimental kinetic measurements (26.9 kcal/mol).

The transition state for reductive elimination resembles a migration of the alkyl ligand to the anilido nitrogen (Figure 7). The P–Pd–C bond angle is computed to increase from 101° to 127°, and the C–Pd–N bond angle to decrease from 95° to 57° during the reaction of complex **8a** to form alkylamine **3i**. Similar results were observed for reductive elimination from the other four-coordinate complexes (see the SI for details). These changes in bond angles are consistent with those previously reported for the reductive elimination of arylamines from phosphine- or NHC-ligated arylpalladium(II) amido complexes.[32–34]

However, the change in the Pd–C bond distance during the reductive elimination of alkylamines is much different from that during reductive elimination to form arylamines and leads to the description of a process involving migration of the alkyl group to nitrogen. The Pd–C bond length in complex **8a** is computed to increase from 2.09 Å in the ground state to 2.46 Å in the transition state, whereas the Pd–N distance is computed to remain roughly constant (2.06 Å) (Figures 6 and 7). A similar change of 0.34 Å in the Pd–C bond distance was reported in our prior communication on reductive elimination from NHC-ligated *syn*-3-methylnorborn-2-yl amido complexes.[14] Much smaller changes in the Pd–C bond (<0.1 Å) were computed to occur during the reductive eliminations of arylamines from arylpalladium(II) amido complexes in previous work.[32–34] Thus, our computations suggest that the Pd–C bond in the transition state to form alkylamines is weaker than that in the transition state to form arylamines.

The distances from the palladium to the coordinated oxygen (Pd–O) are calculated to increase along the reaction coordinate from the ground states to the transition states (Figure 7, Table 4). The average increase in the Pd–O bond length for the complexes **8a**–**d** containing rigid 2-methoxyaryl groups on the phosphine was only 17% of the starting bond length (Table 4, entries 1–4). These Pd–O distances are all significantly less than the sum of the van der Waals radii (1.63 and 1.52 Å for Pd and O, respectively).[35] The calculated free energy barriers for this pathway agreed well with those measured experimentally (Tables 3 and 4). Therefore, computations suggest that reductive elimination occurs directly from the four-coordinate complexes and through a four-coordinate transition state (Figure 7).

The flexibility of the 2-methoxyethyl group in complex **8e** creates the possibility that isomerization occurs to form a three-coordinate species. An isomeric κP ground state structure (**9**) was located in which the O donor of the P,O ligand has dissociated from the palladium center (Figure 6). This dissociation step was calculated to be both exergonic and fast, with $\Delta G = -0.8$ kcal/mol and $\Delta G^{\ddagger} = 3.2$ kcal/mol (relative to **8e**) (Figure 8). Furthermore, a conformer of **9** (related by rotation of the P–Pd bond) was found, and the calculated energy of this conformer was 0.9 kcal/mol lower than the energy of **9** (complex **9′**, Figure 6). Therefore, **8e** could isomerize to a three-coordinate species prior to reductive elimination. However, neither complex **9′** nor other three-coordinate isomers were observed experimentally by NMR spectroscopy. The many possible conformers of **9**

complicate the process of predicting the lowest energy species by DFT, and the similarity in energy between these four-coordinate and three-coordinate complexes suggests that both may be relevant to the mechanism of reductive elimination from complexes bearing the 2-methoxyethylphosphine ligand.

To gain more information from computation about the relationship between the flexibility of the ancillary ligand and the rate of reductive elimination, the pathway for simultaneous dissociation and reductive elimination of the amine and the pathway for reductive elimination after dissociation of the ether oxygen to form **9** were evaluated. A transition state for reductive elimination directly from the κ^2*P,O* complex **8e** was found and was 23.1 kcal/mol above the ground state (Table 4, entry 5). In contrast to the change in Pd–O bond distance during formation of the transition state for the reaction of **8a** bearing the rigid *o*-anisylphosphine, the increase in the Pd–O distance during the reaction of complex **8e** containing the flexible 2-methoxyethyl group is large (approximately 57% of the starting bond length). The Pd–O distance in the transition state for reductive elimination from **8e** is longer than what can be considered a bond; the value of 3.87 Å is substantially greater than the sum of the van der Waals radii (3.15 Å).[36] Thus, reductive elimination and dissociation of the ether occur simultaneously to generate this transition state. In addition, the transition states for reductive elimination from the κ*P* isomers **9** and **9′** were found, and the energies of these transition states were 0.9 and 1.1 kcal/mol lower, respectively, than that of the transition state for the reaction of **8e** (Figure 8). The differences in calculated barriers between these three pathways are likely less than the error in the calculations. Therefore, these computational results strongly suggest that reductive elimination from **8e** occurs with dissociation of the oxygen from the palladium center, but they cannot distinguish clearly between pathways by which dissociation occurs prior to or in concert with reductive elimination. These calculations indicate that the relative stabilities of κ^2*P,O* and κ*P* isomers of complexes bearing flexible P,O ligands will affect the rate of reductive elimination.

The computed and experimentally measured barriers to reductive elimination from 2-methoxyethyl-ligated **8e** were lower than those from the analogous methoxyaryl-ligated **8b** (Tables 3 and 4). This difference in reactivity is unlikely to result from differences in the steric or electronic properties of the phosphine because the differences in steric properties are small (Table 4, Figure 4, Figure 5, and Figure 6), and the greater electron donation by the ligand in **8e** than by the ligands in **8a**–**b** should lead to an increase in the barrier to reductive elimination. Therefore, we propose that the higher reactivity of **8e** than of **8a** or **8b** is primarily a result of the smaller energy required for the flexible ether ligand in **8e** to dissociate from the metal center during reductive elimination.

The possibility that an interaction between the ether group in the anilido ligand and the palladium center affects the barrier to reductive elimination was evaluated. However, the distances from Pd to the oxygen atoms in the anilido ligands of the transition states for reductive elimination from **8a**–**e** were over4.71 Å. Therefore, the effect of these interactions on the kinetic barrier to reductive elimination is predicted to be small.

Computational Results. 2. Mechanism of Reductive Elimination from Complexes Ligated by t-Bu$_3$P.—The *t*-Bu$_3$P-ligated complexes **2a**–**i** were too unstable

to isolate and characterize by X-ray diffraction. Therefore, the computed structure of the ground state of the three-coordinate, *t*-Bu_3P-ligated alkylpalladium(II) amido complex **2a** bearing a phenyl group on nitrogen was obtained by altering the structure of the four-coordinate, *t*-Bu_2(*o*-anisyl)P-ligated Pd(II) anilido complex **8a** (Figure 9). The *ortho*-anisyl group on phosphorus in this complex was replaced by a third *tert*-butyl group, and the 4-fluoro-2-methoxyphenyl group on nitrogen was replaced with a phenyl group. The energy of the resulting structure was then minimized, and the structures of the other *t*-Bu_3P-ligated complexes **2b**–**i** were obtained by introducing the appropriate substituents on the aryl group and minimizing the energy.

The transition state structures for reductive elimination of alkylamines **3a**–**i** from *t*-Bu_3P-ligated Pd(II) amido complexes **2a**–**i** were computed (Figure 9 and Table 5). The average computed free energy barrier for reductive elimination of *para*- and *meta*-substituted amines **3a**–**g** was 22.9 ± 0.7 kcal/mol (entries 1–7). This average computed free-energy barrier agrees well with the average experimental free-energy barrier of 23.4 ± 0.6 kcal/mol (Table 2, entries 1–7) for reductive elimination from the same complexes. However, the experimentally observed correlation between the electronic properties of the anilido ligand and the rate of reductive elimination from **2a**–**g** presented in Table 2 and Figure 1 was not well reproduced by DFT, most likely because the variations in computed barriers between these complexes are within the accuracy of the calculations.

The computational results suggest that conformational effects may contribute substantially to the rate of reductive elimination. The barriers to reductive elimination from conformers (related by rotation of the C–N bond) of *meta*- and *ortho*-substituted complexes **2e**–**i** were computed, and this rotation was found to have a significant effect on the barrier to reductive elimination. In the cases of complexes **2e** and **2g**, reductive elimination is calculated to occur after rotation of the C–N bond; the lower-energy transition state corresponds to the higher-energy ground state. Rotation of the C–N bond in *ortho*-substituted **2h** and **2i** was predicted to be endergonic by7.3 and 4.2 kcal/mol, respectively. The computed free energy barriers to reductive elimination from the more sterically encumbered, *ortho*-substituted **2h** and **2i** (25.2 and 23.4 kcal/mol, respectively) agreed exceptionally well with those measured experimentally (25.5 and 23.5 kcal/mol, Table 2). The general agreement between the computed barriers and experimentally measured barriers for reactions from palladium(II) amido complexes containing a *t*-Bu_3P ancillary ligand further supports the conclusion that the reaction occurs by a concerted pathway for reductive elimination to form alkyl–nitrogen bonds.

CONCLUSIONS

We have shown that reductive elimination to form sp^3 C–N bonds by a concerted pathway can occur with low barriers from monomeric three-coordinate phosphine-ligated (*syn*-3-methylnorborn-2-yl)palladium(II) complexes and from four-coordinate analogs containing chelating ligands comprising one phosphine that is strongly electron donating and one ether that is weakly electron donating. An analysis of the factors controlling the rate of reductive elimination revealed that the fastest reductive eliminations occurred from complexes bearing unhindered and electron-rich anilido ligands. The same trend was observed for reactions of

the *t*-Bu_3P-ligated alkylpalladium(II) complexes reported herein as for the analogous NHC-ligated complexes previously reported in communication form[14] and for arylpalladium(II) complexes that undergo reductive elimination of arylamines.[1,37] DFT calculations predict that conformational effects, such as rotation around the C–N bond, also have a significant impact on the rate of reductive elimination.

Syn-3-methylnorborn-2-ylpalladium(II) anilido complexes containing monophosphines smaller than *t*-Bu_3P form bimetallic structures containing one phosphine and one bridging anilide as the dominant species in solution. Kinetic experiments conducted with added phosphine suggest that reductive elimination from this bimetallic complex occurs via reversible formation of a three-coordinate monometallic species. Our results indicate that this reaction is reversible when phosphine is present in high concentrations. However, the unproductive formation of anilide-bridged bimetallic complexes would likely limit the utility of these complexes as catalysts in the development of new synthetic methods for the production of alkylamines.

Four-coordinate Pd(II) anilido complexes containing neutral, bidentate 2-methoxyarylphosphine (P,O) ligands are monometallic and stable at ambient temperature, but they undergo reductive elimination at mild temperatures. The barriers to reductive elimination from these four-coordinate complexes are1.6 to 3.2 kcal/mol higher than that for reductive elimination from the analogous three-coordinate, *t*-Bu_3P-ligated complex. Computations indicate that complexes of the rigid P,O ligands undergo reductive elimination directly from the four-coordinate complexes, but the palladium–oxygen bond lengthens significantly from the ground state to the transition state.

The reductive eliminations from complexes ligated by 2-methoxyaryl phosphines bearing electron-withdrawing groups were faster than those from complexes ligated by unsubstituted, *o*-anisylphosphines. Furthermore, the reductive eliminations from the *t*-Bu_3P-ligated complexes are approximately 40 times faster than those from the analogous, more electron-rich NHC-ligated complexes,[38] corresponding to a difference in free energy of activation of approximately 2.7 kcal/mol. These results are consistent with the trend that reductive elimination occurs more rapidly from more electron-deficient complexes than from more electron-rich complexes, which is consistent with the trends reported for other classes of concerted reductive eliminations from Pd(II).[22]

Complexes containing chelating ligands with flexible backbones have been shown to undergo reductive elimination to form C–C bonds faster than those with more rigid backbones. Goldberg and co-workers have reported that the rates of reaction to form sp^3 C–C bonds from (P,P)Pt(IV)Me_4 complexes ligated by flexible bisphosphines are faster than the rates of the same reaction from complexes containing ligands with equal bite angles but more rigid linkers.[39,40] The authors proposed that reductive elimination occurs via initial dissociation of one phosphine donor to form a pentacoordinate intermediate, and that the energy difference between hexa- and pentacoordinate structures is smaller for complexes ligated by flexible bisphosphine ligands than for complexes ligated by more rigid bisphosphines.[41,42]

We have shown that this trend can be taken even further by combining the effects of flexibility in the linker with weak donation by an ether. The four-coordinate (κ^2-*P,O*) and three-coordinate (κ-*P*) isomers of an alkylpalladium(II) anilido complex bearing the flexible P,O ligand $Ad_2PCH_2CH_2OCH_3$ are computed to be similar in energy, and the reductive elimination reaction from this complex is faster and higher yielding than that from the analogous complex containing a rigid linker. Computations suggest that the rigid, aryl backbones in *ortho*-anisyl phosphines do not allow for dissociation of the ether to form the three-coordinate isomer. We suggest that the effects of weak chelation on the mechanism of reductive elimination could be elements of design for catalysts that react by reductive elimination to form alkyl–nitrogen bonds.

The trends revealed by the current work suggest strategies to increase the rate of reductive elimination and to prevent unproductive decomposition pathways. Specifically, we have shown that coordination by P,O bidentate ligands can stabilize reactive Pd(II) anilido intermediates without significantly decreasing the yields from reductive elimination. The square planar structures of these complexes are expected to lead to higher barriers to unproductive decomposition pathways, such as β-hydride elimination. Furthermore, chelation should disfavor decomposition pathways involving phosphine dissociation or formation of bimetallic, anilide-bridged complexes. Therefore, we expect that ligand structures like those in Schemes 5 and 6 will enable an expansion of the scope of alkyl and amido groups that undergo reductive elimination.

Supplementary Material

Refer to Web version on PubMed Central for supplementary material.

ACKNOWLEDGMENTS

The authors gratefully acknowledge funding from the National Science Foundation Center for Enabling New Technologies through Catalysis (Grant CHE-1205189). X-ray diffraction crystallography was performed by Dr. Antonio DiPasquale at the UC Berkeley CheXRay facility (NIH S10-RR027172). We thank Dr. Hasan Celik at the UC Berkeley NMR Facility for his assistance with DOSY and ^{1}H-^{31}P HMBC NMR spectroscopy experiments. T.R.C. and Q.J. also acknowledge the National Science Foundation for their support of the UNT Chemistry CASCaM high performance computing facility through Grant CHE-1531468.

REFERENCES

(1). Driver MS; Hartwig JF J. Am. Chem. Soc 1997, 119 (35), 8232–8245.

(2). Yamashita M; Hartwig JF J. Am. Chem. Soc 2004, 126 (17), 5344–5345. [PubMed: 15113190]

(3). Pendleton IM; Pérez-Temprano MH; Sanford MS; Zimmerman PM J. Am. Chem. Soc 2016, 138 (18), 6049–6060. [PubMed: 27087364]

(4). Pérez-Temprano MH; Racowski JM; Kampf JW; Sanford MS J. Am. Chem. Soc 2014, 136 (11), 4097–4100. [PubMed: 24579653]

(5). Camasso NM; Canty AJ; Ariafard A; Sanford MS Organometallics 2017, 36 (22), 4382–4393.

(6). Koo K; Hillhouse GL Organometallics 1995, 14 (9), 4421–4423.

(7). Pawlikowski AV; Getty AD; Goldberg KI J. Am. Chem. Soc 2007, 129 (34), 10382–10393. [PubMed: 17672451]

(8). Rucker RP; Whittaker AM; Dang H; Lalic GJ Am. Chem. Soc 2012, 134 (15), 6571–6574.

(9). Lin BL; Clough CR; Hillhouse GL J. Am. Chem. Soc 2002, 124 (12), 2890–2891. [PubMed: 11902877]

(10). Catellani M; Del Rio A Russ. Chem. Bull 1998, 47 (5), 928–931.

(11). Lautens M; Paquin JF; Piguel S; Dahlmann MJ Org. Chem 2001, 66 (24), 8127–34.

(12). Pan J; Su M; Buchwald SL Angew. Chem., Int. Ed 2011, 50(37), 8647–8651.

(13). Marquard SL; Rosenfeld DC; Hartwig JF Angew. Chem., Int. Ed 2010, 49 (4), 793–796.

(14). Hanley PS; Marquard SL; Cundari TR; Hartwig JF J. Am. Chem. Soc 2012, 134 (37), 15281–15284. [PubMed: 22934822]

(15). Low JJ; Goddard WA J. Am. Chem. Soc 1986, 108 (20), 6115–6128.

(16). Mann G; Shelby Q; Roy AH; Hartwig JF Organometallics 2003, 22 (13), 2775–2789.

(17). Attempts to isolate a crystalline sample of complex **6a** were unsuccessful.**6a**

(18). Tolman CA Chem. Rev 1977, 77 (3), 313–348.

(19). The substituent contributions to the Tolman electronic paramater are 0, 4.3, and, 0.1 for t-Bu, Ph, and Cy, respectively.

(20). DiCosimo R; Whitesides GM J. Am. Chem. Soc 1982, 104(13), 3601–3607.

(21). Tatsumi K; Nakamura A; Komiya S; Yamamoto A; Yamamoto TJ Am. Chem. Soc 1984, 106 (26), 8181–8188.

(22). Hartwig JF Inorg. Chem 2007, 46 (6), 1936–1947. [PubMed: 17348724]

(23). Gusev DG Organometallics 2009, 28 (22), 6458–6461.

(24). Kelly Iii RA; Clavier H; Giudice S; Scott NM; Stevens ED; Bordner J; Samardjiev I; Hoff CD; Cavallo L; Nolan SP Organometallics 2008, 27 (2), 202–210.

(25). We also synthesized the complex [Ad2PCH2(2-(5-BrC5H3N))]-Pd(3-CH3norborn-2-yl)(Cl) to test whether decreasing the basicity of the pyridine donor would enable reductive elimination to occur. However, only trace formation of **3i** was detected in reactions of this complex (see the SI for details).**3i**

(26). Frisch MJ; Trucks GW; Schlegel HB; Scuseria GE; Robb MA; Cheeseman JR; Scal-mani G; Barone V; Mennucci B; Petersson GA; Nakatsuji H; Caricato M; Li X; Hratchian HP; Izmaylov AF; Bloino J; Zheng G; Sonnenberg JL; Hada M; Ehara M; Toyota K; Fukuda R; Hasegawa J; Ishida M; Nakajima T; Honda Y; Kitao O; Nakai H; Vreven T; Montgomery JA Jr.; Peralta JE; Ogliaro F; Bearpark M; Heyd JJ; Brothers E; Kudin KN; Staroverov VN; Kobayashi R; Normand J; Raghavachari K; Rendell A; Burant JC; Iyengar SS; Tomasi J; Cossi M; Rega N; Millam JM; Klene M; Knox JE; Cross JB; Bakken V; Adamo C; Jaramillo J; Gomperts R; Stratmann RE; Yazyev O; Austin AJ; Cammi R; Pomelli C; Ochterski JW; Martin RL; Morokuma K; Zakrzewski VG; Voth GA; Salvador P; Dannenberg JJ; Dapprich S; Daniels AD; Farkas O; Foresman JB; Ortiz JV; Cioslowski J; Fox DJ Gaussian 09, revision D.01; Gaussian, Inc.: Wallingford, CT, 2013.

(27). Becke AD J. Chem. Phys 1993, 98 (7), 5648–5652.

(28). Cundari TR; Stevens WJ J. Chem. Phys 1993, 98 (7), 5555–5565.

(29). Stevens WJ; Basch H; Krauss MJ Chem. Phys 1984, 81(12), 6026–6033.

(30). Stevens WJ; Krauss M; Basch H; Jasien PG Can. J. Chem 1992, 70 (2), 612–630.

(31). Marenich AV; Cramer CJ; Truhlar DG J. Phys. Chem. B 2009, 113 (18), 6378–6396. [PubMed: 19366259]

(32). Cundari TR; Deng JJ Phys. Org. Chem 2005, 18 (5), 417–425.

(33). Hoi KH; Çalimsiz S; Froese RDJ; Hopkinson AC; Organ MG Chem. - Eur. J 2012, 18 (1), 145–151. [PubMed: 22139675]

(34). Klinkenberg JL; Hartwig JF J. Am. Chem. Soc 2010, 132(34), 11830–11833. [PubMed: 20695642]

(35). Bondi AJ Phys. Chem 1964, 68 (3), 441–451.

(36). Attempts to locate a transition state structure in which the Pd–O distance is within the sum of the VdW radii were unsucessful.

(37). Yamashita M; Cuevas Vicario JV; Hartwig JF J. Am. Chem. Soc 2003, 125 (52), 16347–16360. [PubMed: 14692777]

(38). The rate constants for reductive elimination of **2b** and **2c** were calculated at 363 K, assuming an entropy of activation of −14 eu. Solvent effects are expected to be small.**2b2c**

(39). Arthur KL; Wang QL; Bregel DM; Smythe NA; O'Neil BA; Goldberg KI; Moloy KG Organometallics 2005, 24(19), 4624–4628.

(40). Crumpton-Bregel DM; Goldberg KI J. Am. Chem. Soc 2003, 125 (31), 9442–9456. [PubMed: 12889975]

(41). Brown MP; Puddephatt RJ; Upton CEEJ Chem. Soc., Dalton Trans 1974, 22, 2457–2465.

(42). Roy S; Puddephatt RJ; Scott JDJ Chem. Soc., Dalton Trans 1989, 11, 2121–2125.

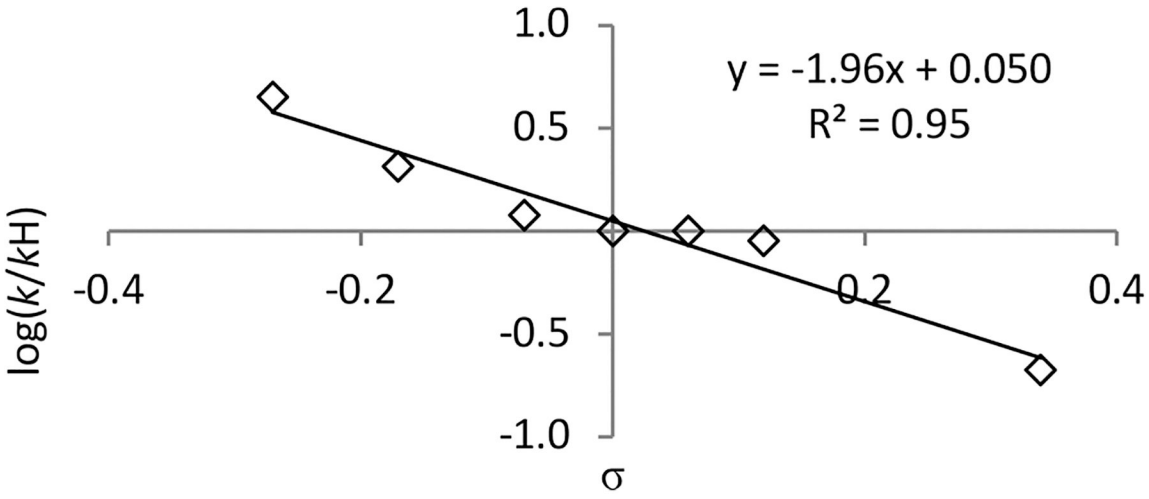

Figure 1.
Hammett plot for substituent effects on the anilido ligand. Data from entries 1–7 of Table 2.

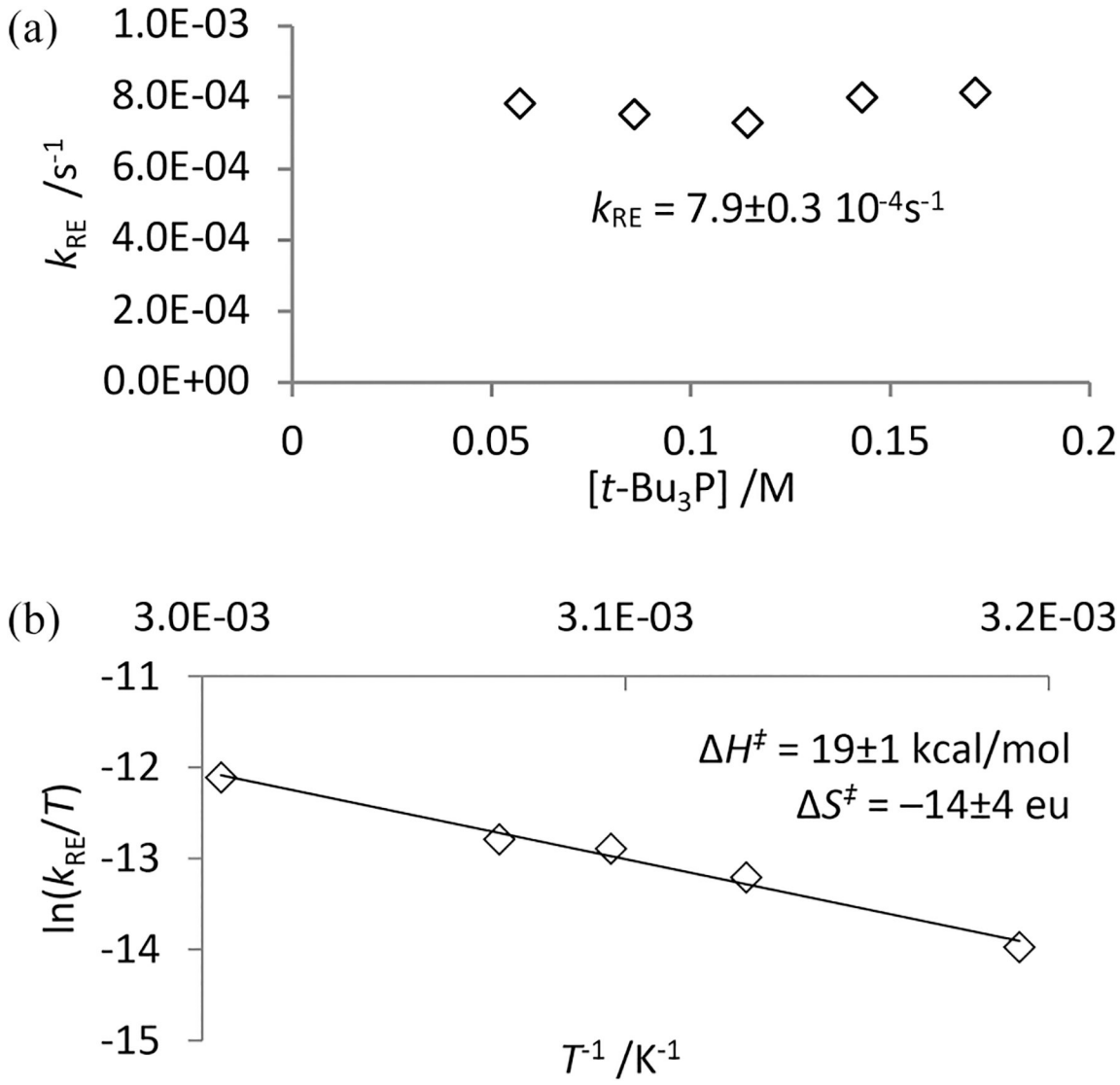

Figure 2.

Determination of the order in [t-Bu$_3$P] and activation parameters for reductive elimination from **2i**. Solutions of **2i** were prepared as described in Scheme 2. (a) Equivalents of t-Bu$_3$P were varied from 1 to 3 with T = 323 K. (b) T was varied from 313 to 333 K with 3 equiv of t-Bu$_3$P.

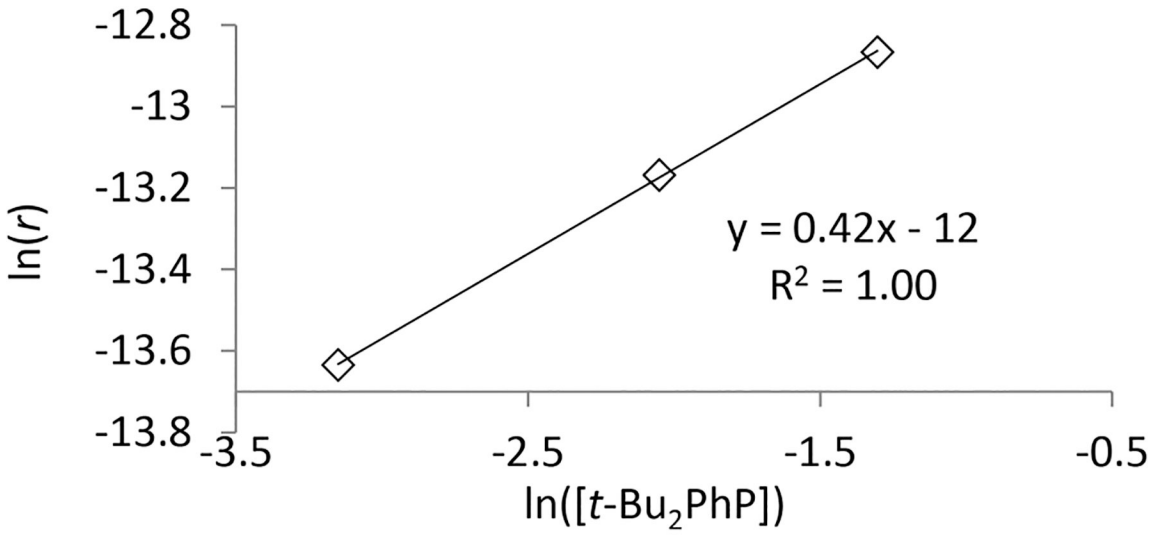

Figure 3.

Effect of the concentration of *t*-Bu_2PhP on the rate of formation (*r*) of **3i**. Experiments were performed at 50 °C in THF. Concentrations of **3i** were measured by ^{19}F NMR spectroscopy with 4-FTol as internal standard. Initial rates were measured as the slope of a linear fit of [**3i**] vs time plot for <15% yield.

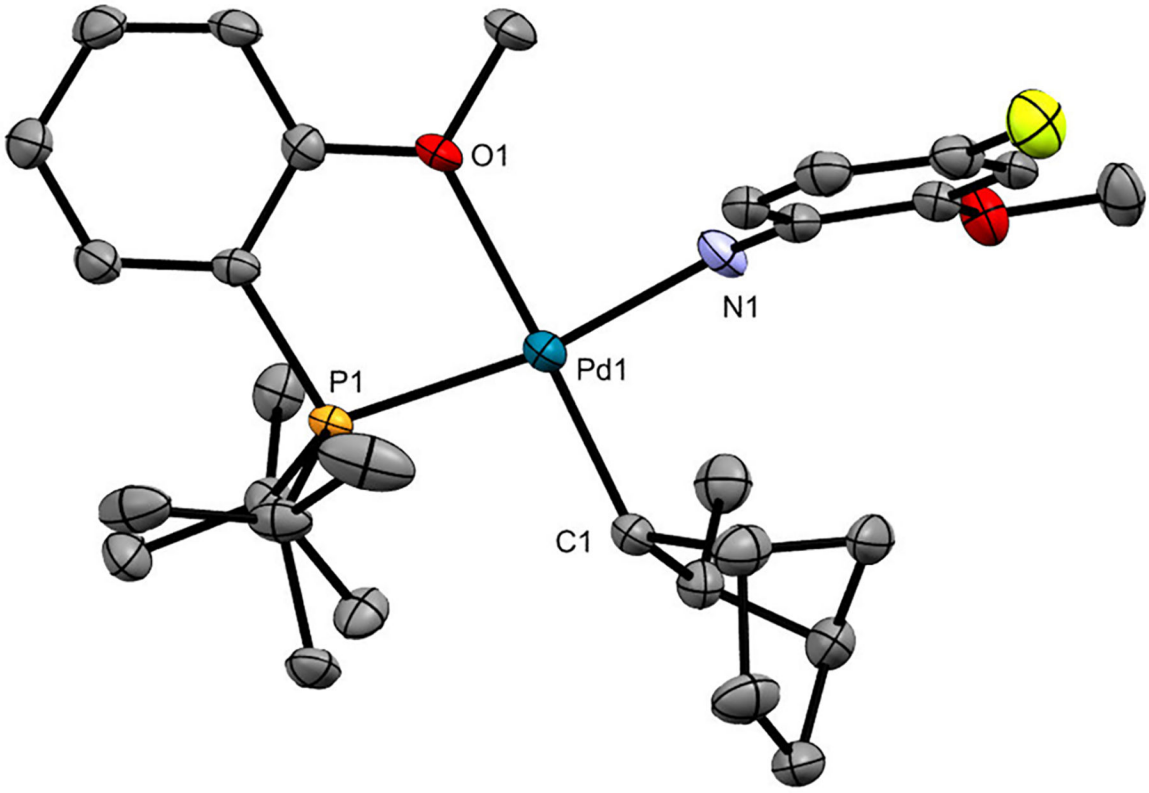

Figure 4.

ORTEP drawing of [*t*-Bu_2(*o*-anisyl)P-κ^2*P,O*]Pd(3-CH_3norborn-2-yl)NHAr **8a** with 50% probability ellipsoids. Hydrogen atoms are omitted for clarity. Selected bond lengths (Å) and angles (deg) for **8a**: Pd1–O1 2.288(2), Pd1–P1 2.2881(8), Pd1–C1 2.057(3), Pd1–N1 2.053(3); O1–Pd1–P1 80.40(6), P1–Pd1–C1 97.38(9), C1–Pd1–N1 92.92(12), N1–Pd1–O1 89.32(9). For the analogous bonds in **8b**: Pd1–O1 2.2829(16), Pd1–P1 2.2954(6), Pd1–C1 2.058(2), Pd1–N1 2.0479(19); O1–Pd1–P1 80.62(4), P1–Pd1–C1 99.69(7), C1–Pd1–N1 91.19(9), N1–Pd1–O1 88.46(7).

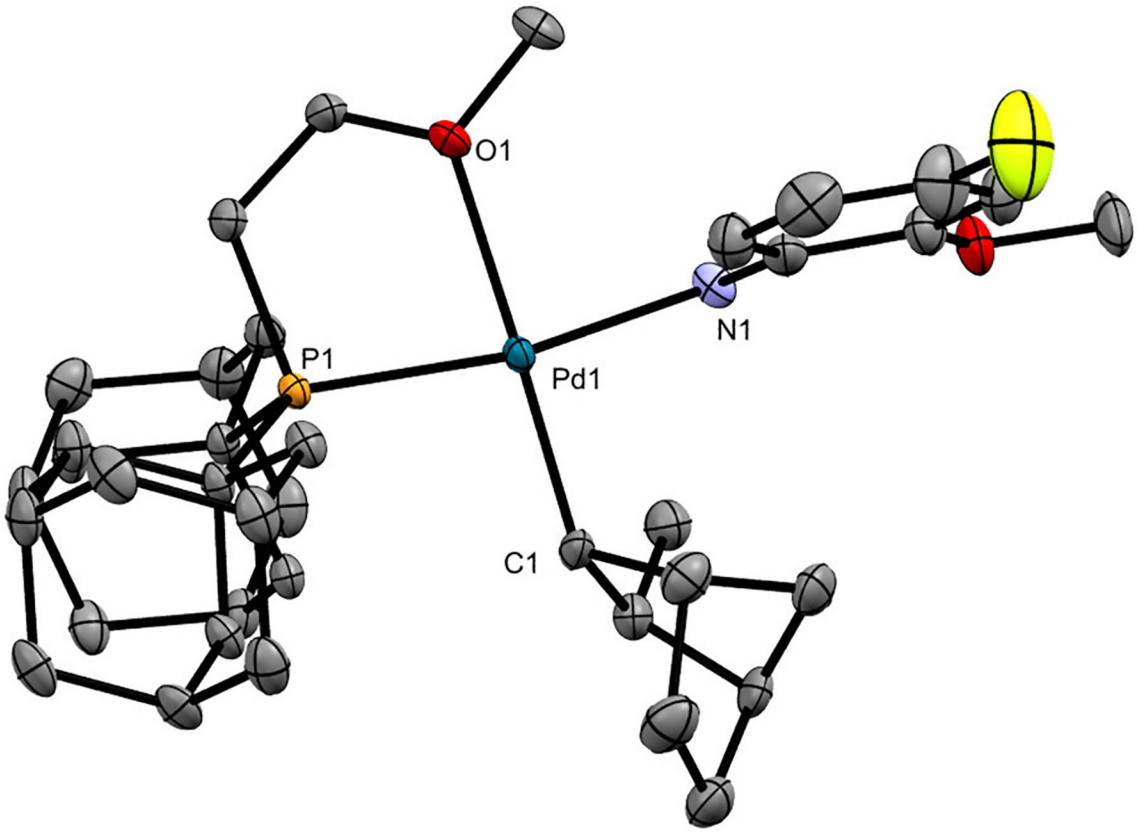

Figure 5.

ORTEP drawing [$Ad_2PCH_2CH_2OCH_3$-κ^2*P,O*]Pd(3-CH_3norborn-2-yl)NHAr **8e** with 50% probability ellipsoids. Hydrogen atoms are omitted for clarity. Selected bond lengths (Å) and angles (deg): Pd1–O1 2.297(2), Pd1–P1 2.2898(9), Pd1–C1 2.042(4), Pd1–N1 2.081(3); O1–Pd1–P1 81.79(6), P1–Pd1–C1 97.24(10), C1–Pd1–N1 92.98(13), N1–Pd1–O1 88.48(10).

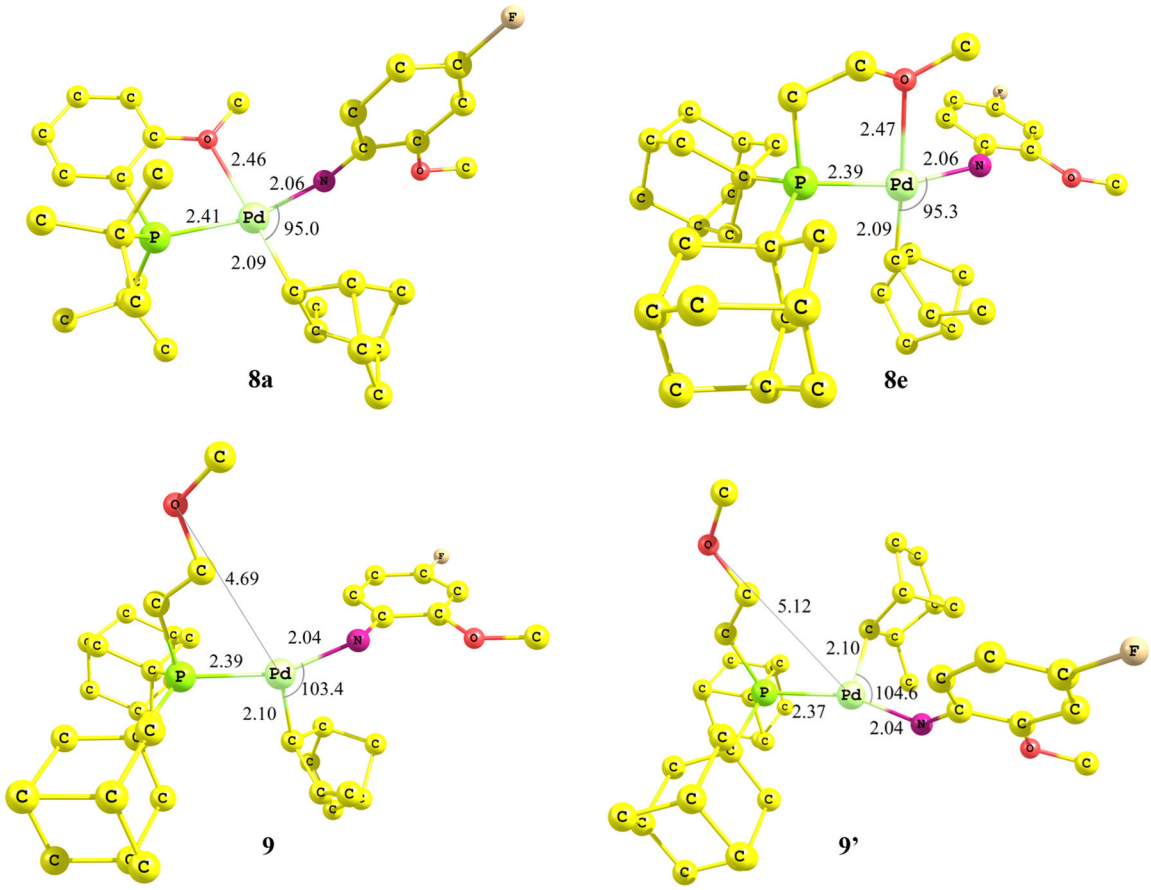

Figure 6.

Computed ground state structures for [*t*-Bu_2(*o*-anisyl)P-κ^2*P,O*]Pd(3-CH_3norborn-2-yl)NHAr **8a** and [$Ad_2PCH_2CH_2OCH_3$-κ^2*P,O*]Pd(3-CH_3norborn-2-yl)NHAr **8e**, and [$Ad_2PCH_2CH_2OCH_3$-κ*P*]Pd(3-CH_3norborn-2-yl)NHAr **9** and **9′**. Bond lengths in Å, bond angles in degrees. Hydrogen atoms are omitted for clarity.

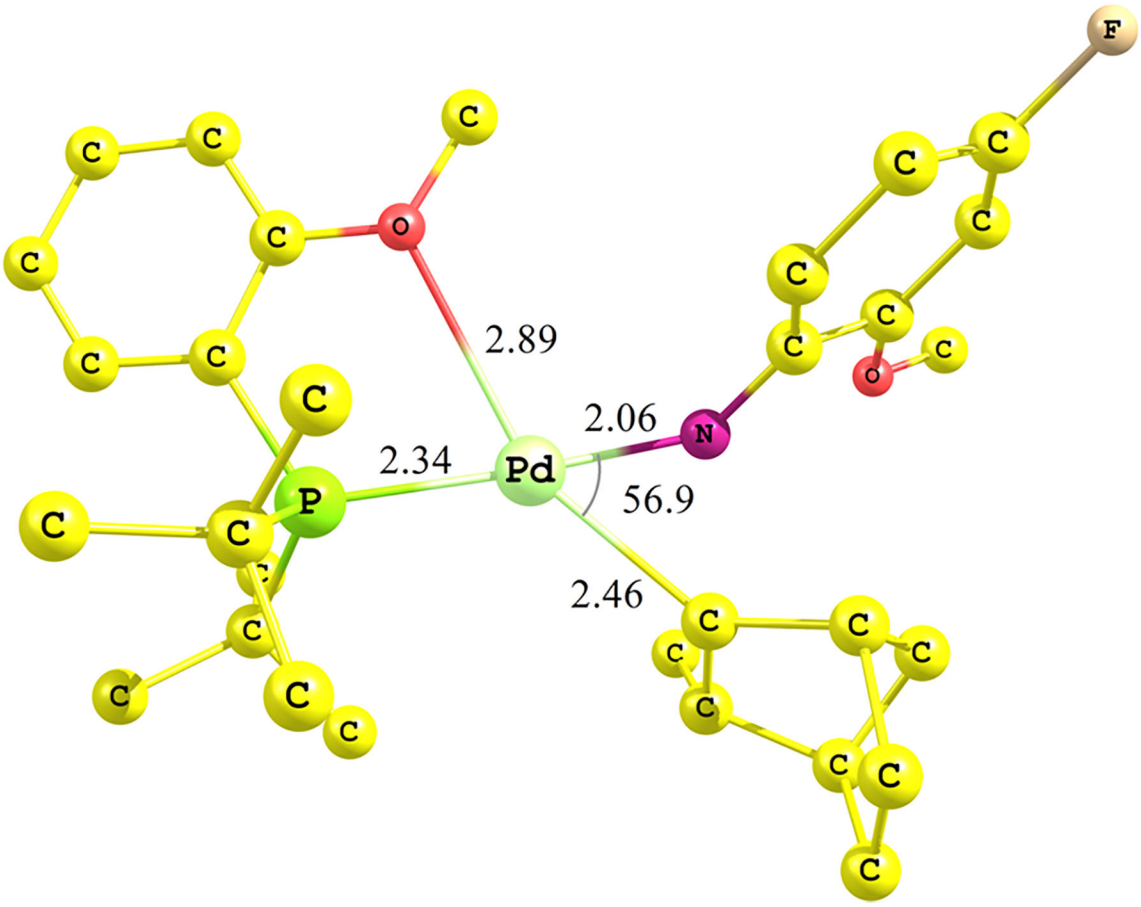

Figure 7.

Computed transition state structure for reductive elimination of norbornylamine **3i** from [*t*-Bu_2(*o*-anisyl)P]Pd(3-CH_3norborn-2-yl)NHAr **8a**. Bond lengths in Å, bond angles in degrees. Hydrogen atoms are omitted for clarity.

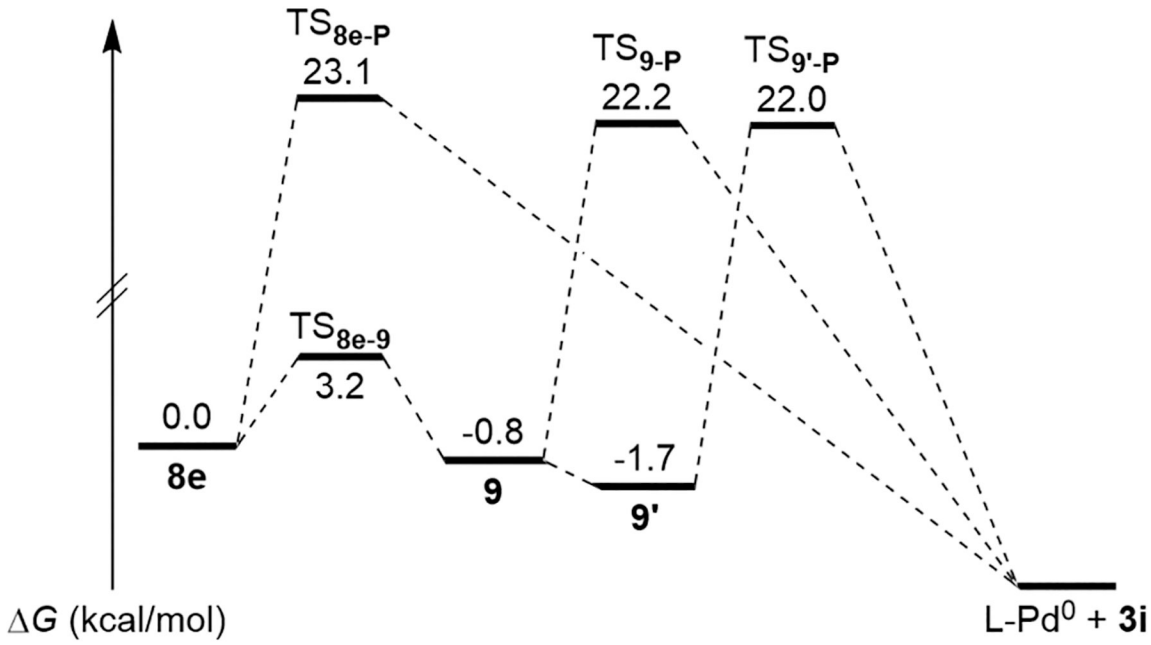

Figure 8.
Free energy profile of three possible reductive elimination pathways. Relative energies are reported at 338 K.

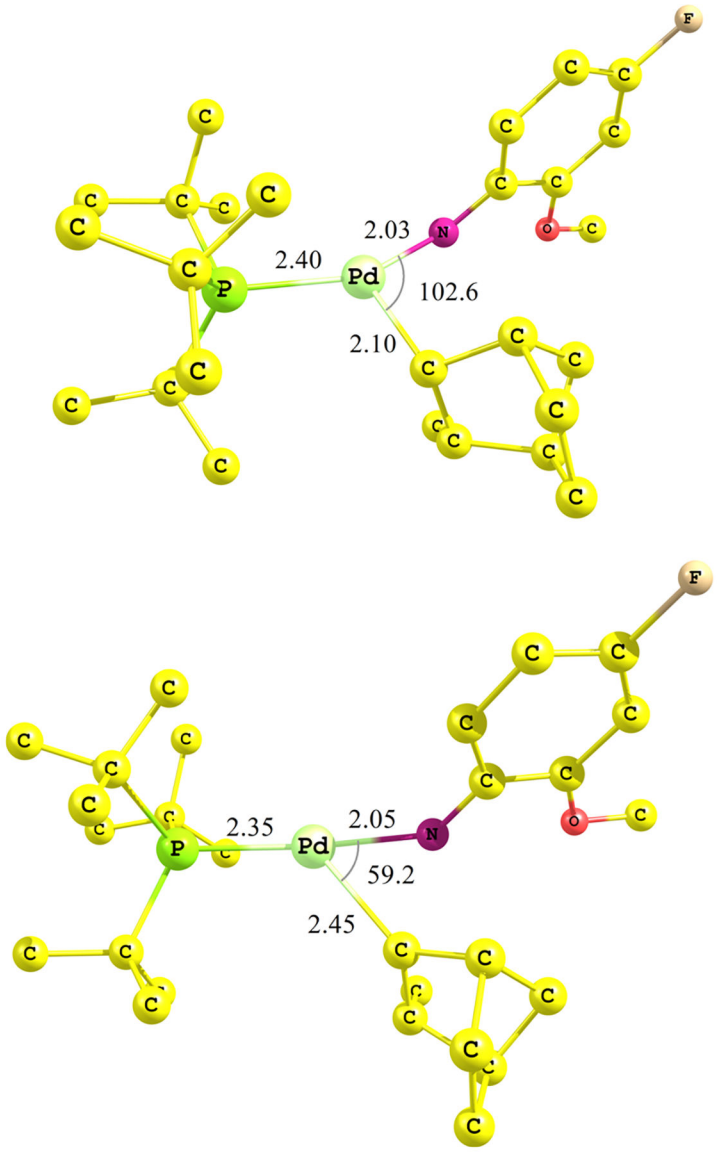

Figure 9.

Computed ground state structure (top) and transition state structure (bottom) of (*t*-Bu_3P)Pd(3-CH_3norborn-2-yl)NHAr **2i**. Bond lengths in Å, bond angles in degrees. Hydrogen atoms are omitted for clarity.

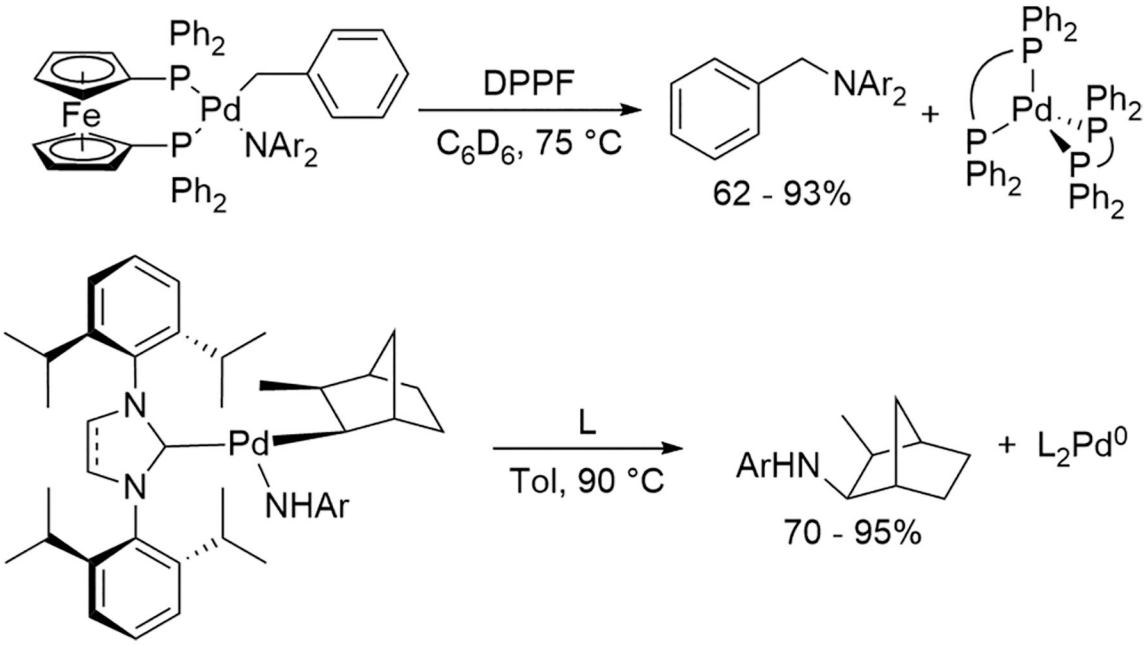

Scheme 1.

Previous Reports of Reductive Elimination of Alkylamines from Pd(II) Anilido Complexes

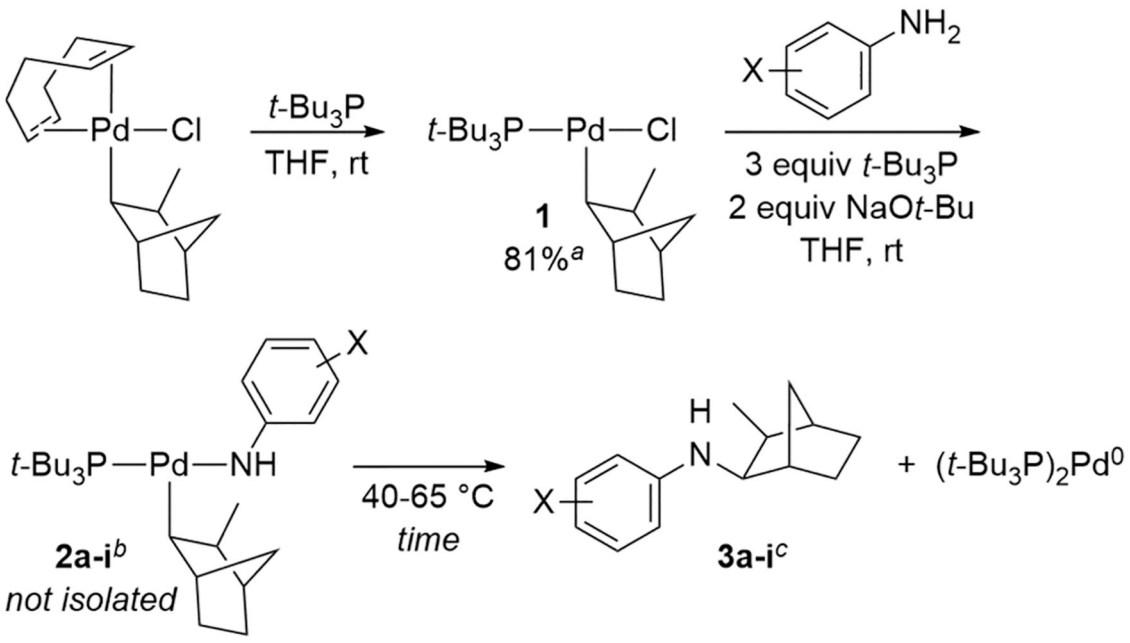

	X	% yield **2a-i**[d]	*time* /h	% yield **3a-i**[d]
a	H	88	5	85 (75)
b	4-OMe	76	1	92 (70)
c	4-Me	89	2	88 (78)
d[e]	4-F	84	5	89 (75)
e	3-Me	92	5	93 (86)
f	3-OMe	85	6	91 (77)
g[e]	3-F	85	40	76 (65)
h[f]	2-*t*-Bu	86	6 (65 °C)	59 (51)
i[e]	4-F-2-OMe	91	4	quant (91)

Scheme 2. Preparation of (*t*-Bu$_3$P)Pd(3-CH$_3$norborn-2-yl)NHAr 2a–i and Reductive Elimination To Form Alkylamines 3a–i

[a]Isolated yield after recrystallization. [b]Conditions unless otherwise noted: Pd–Cl **1** (0.0399 mmol), *t*-Bu$_3$P (0.12 mmol), arylamine (0.042 mmol), and NaO-*t*Bu (0.080 mmol) in THF-d_8 (0.70 mL). [c]Reactions were monitored by ^{1}H NMR spectroscopy while heating at 40 °C in a VT NMR probe for the noted time. [d]Yields determined by ^{1}H NMR spectroscopy with 1,3,5-trimethoxybenzene (TMB) as internal standard (values in parentheses are the overall yields of **3a**–**i** based on **1**); averages from two experiments. [e]Reaction in THF and monitored by ^{19}F NMR spectroscopy with 4-fluorotoluene (4-FTol) as internal standard. [f]Reaction heated at 65 °C.

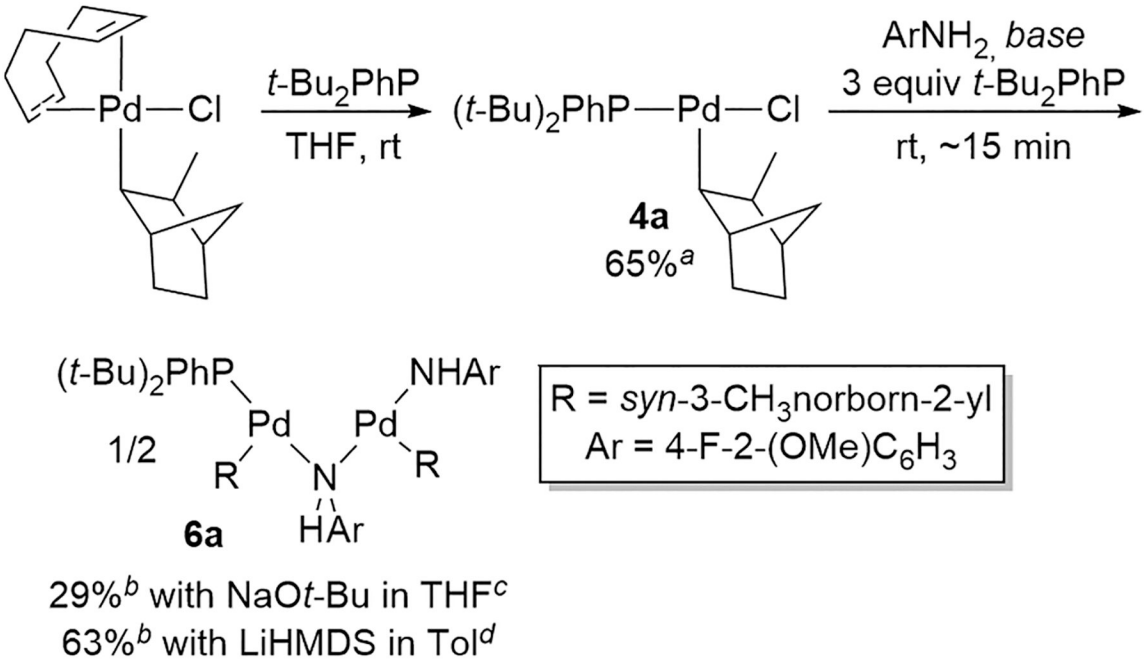

Scheme 3. Formation of Bimetallic Alkylpalladium(II) Amido Complex 6a[a]

[a]Isolated yield after recrystallization. [b]Yield determined by ^{19}F NMR spectroscopy with 4-FTol as internal standard; average from two experiments. [c]Conditions: Pd–Cl **4a** (0.020 mmol), *t*-Bu$_2$PhP (0.060 mmol), 4-fluoro 2-methoxyaniline (0.020 mmol), and NaO*t*-Bu (0.040 mmol) in THF (2.0 mL). [d]Conditions: **4a** (0.010 mmol), *t*-Bu$_2$PhP(0.030 mmol), 4-fluoro 2-methoxyaniline (0.010 mmol), and LiHMDS(0.010 mmol) in Tol (1.0 mL).

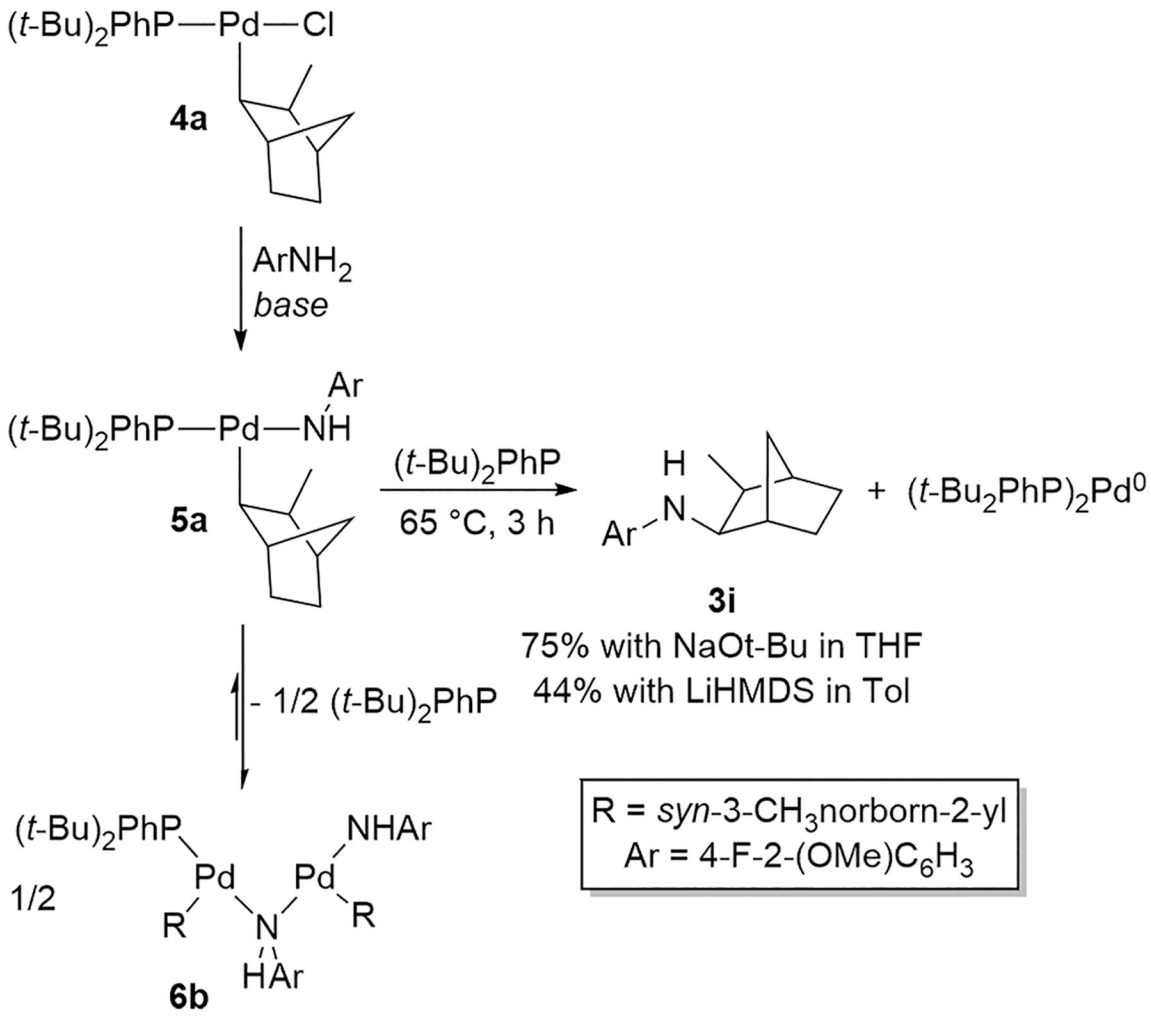

Scheme 4. Reductive Elimination from Bimetallic Alkylpalladium(II) Amido Complex 6a[a]

[a]Samples prepared as described in Scheme 3; yields of **3i** (based on **4a**) determined by ^{19}F NMR spectroscopy with 4-FTol as internal standard; averages from two experiments.

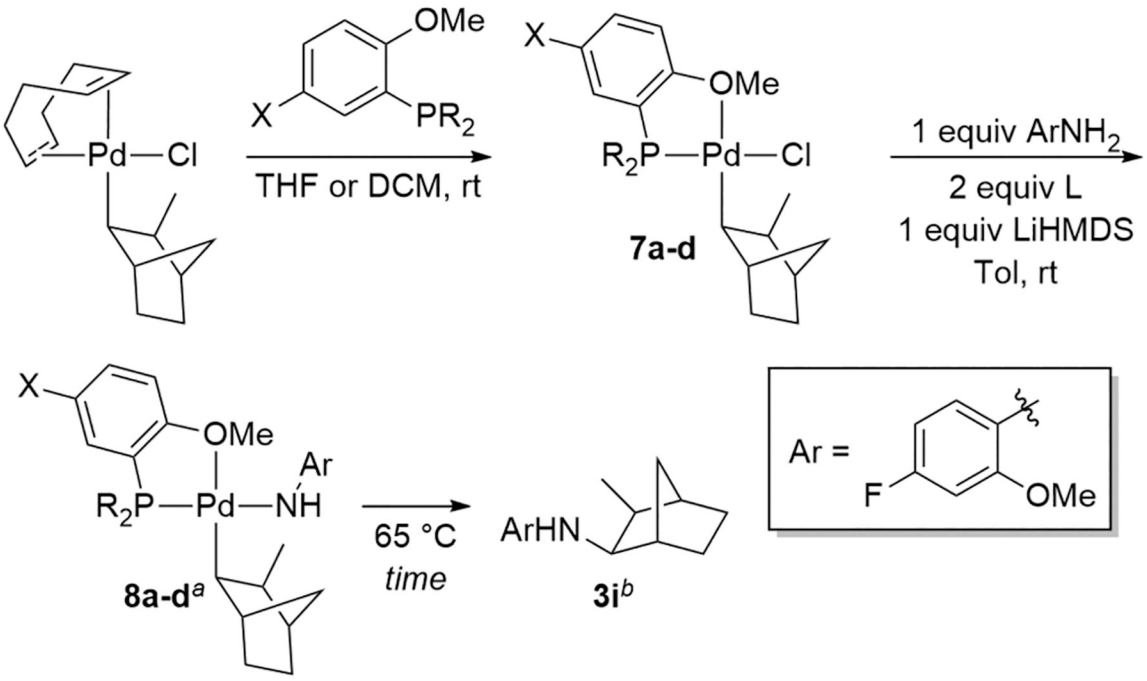

	R	X	% yield **7a-d**[c]	% yield **8a-d**[d]	*time* /h	% yield **3i**[d]
a	*t*-Bu	H	76	88	48	65 (57) 65[e]
b	1-Ad	H	89	85	48	62 (53)
c	*t*-Bu	F	66	87	14	52 (45)
d	*t*-Bu	CF_3	61	89	14	83 (74)

Scheme 5. Preparation of Four-Coordinate [R_2(2-(OMe)Ar)P-κ^2P,O]Pd(3-CH_3norborn-2-yl)NHAr Complexes 8a–d and Reductive Elimination To Form 3i

[a]Conditions: Pd–Cl **7a-d** (0.020 mmol), phosphine (0.040 mmol), 4-fluoro-2-methoxyaniline (0.020 mmol), and LiHMDS (0.020 mmol) in Tol (2.0 mL). [b]The reaction mixture containing **8a**–**d** was heated at 65 °C with stirring in a Teflon-capped vial for the noted time. [c]Isolated yields after recrystallization. [d]Yields determined by ^{19}F NMR spectroscopy with 4-FTol as internal standard (values in parentheses are the overall yield of **3i** based on **7a**–**d**); averages from two experiments. [e]Conditions: isolated **8a** (0.020 mmol) and *t*-Bu_2(*o*-anisyl)P (0.060 mmol) heated at 89 °C for 4 h in Tol-d_8 (0.70 mL).

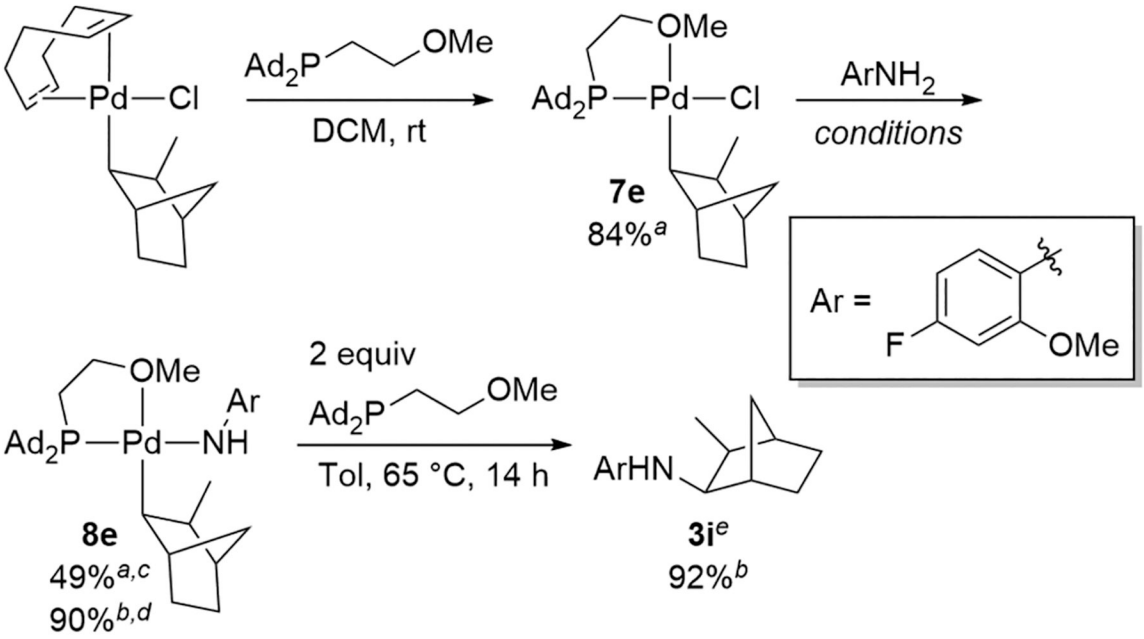

Scheme 6. Preparation of ($Ad_2PCH_2CH_2OCH_3$-κ^2*P,O*)Pd(3-CH_3norborn-2-yl)NHAr (8e) and Reductive Elimination To Form 3i

[a]Isolated yield after recrystallization. [b]Yield determined by ^{19}F NMR spectroscopy with 4-FTol as internal standard; average from two experiments. [c]Conditions: Pd–Cl **7e** (0.134 mmol) and lithium (4-fluoro-2-methoxyphenyl)amide (0.136 mmol) in DCM. [d]Conditions: Pd–Cl **7e** (0.020 mmol), phosphine (0.040 mmol), 4-fluoro-2-methoxyaniline (0.020 mmol), and LiHMDS (0.020 mmol) in Tol (2.0 mL). [e]The reaction mixture containing **8e** and phosphine in toluene prepared as described in footnoted was heated at 65 °C with stirring in a Teflon-capped vial.

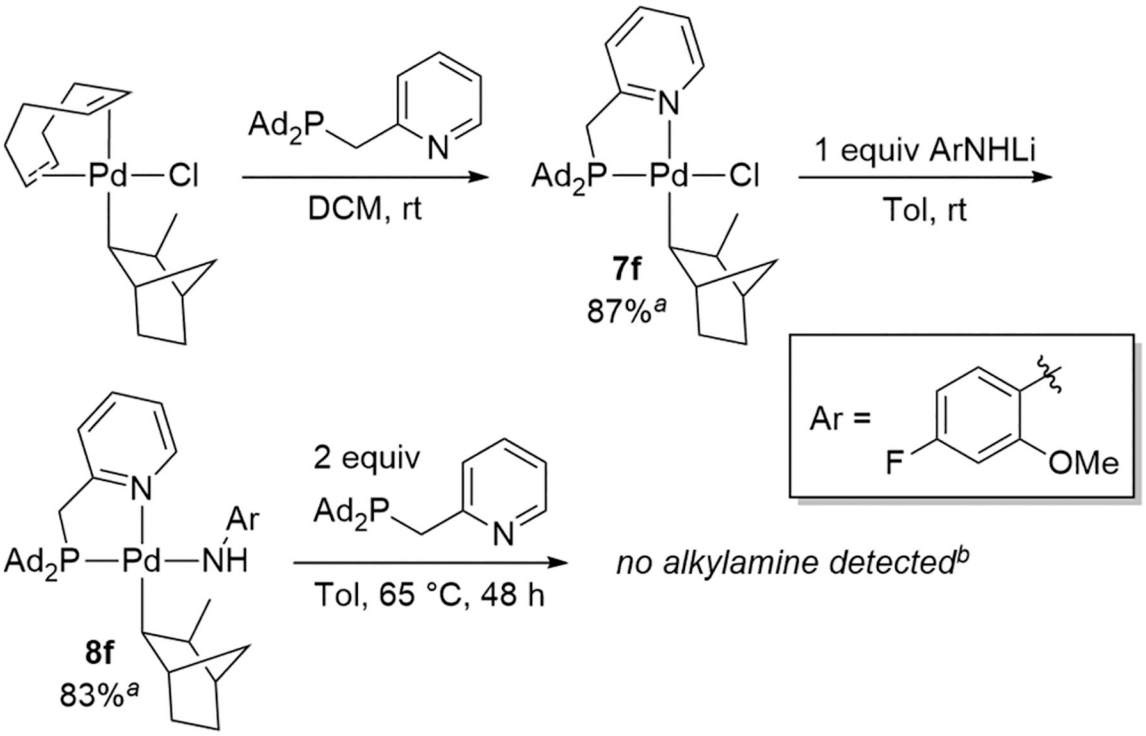

Scheme 7. Preparation of the P,N-Ligated [$Ad_2PCH_2(2\text{-}C_5H_4N)$-$\kappa^2$*P,N*]Pd(3-$CH_3$norborn-2-yl)NHAr (8f)

[a]Isolated yield after recrystallization. [b]By neither GCMS nor ^{19}F NMR spectroscopy; **8f** was also not detected by ^{19}F NMR spectroscopy after heating.

Table 1.

In Situ Molecular Weight Estimation by DOSY[a]

entry	complex	$D \times 10^{10}$ (m^2 s^{-1})	expected *M*	DOSY *M*	error
1	**2g**	12.2	528	497	−31
2	**2i**	12.5	558	527	−31
3	**6**	9.47	934	943	+9
4	**8c**	11.1	626	666	+40

[a]DOSY experiments performed by ^{19}F NMR spectroscopy at 300 K in THF-d_8/THF (~10%). See the SI for details on the calculations of diffusion constants and molecular weight estimates.

Table 2.

Effects of Anilido Substituents on the Rate Constants and Free Energies of Activation for Reductive Eliminations To Form Alkyl–Nitrogen Bonds[a]

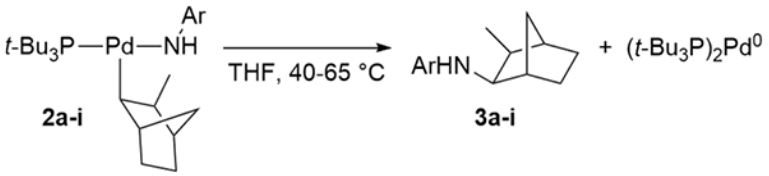

entry	Ar (complex)	$k_{RE}\times10^4$ (s^{-1})	$\Delta G_{RE}^{\ddagger}$ (kcal·mol $^{-1}$)
1	Ph (**2a**)	2.6	23.5
2	4-(OMe)C_6H_4 (**2b**)	12	22.6
3	*p*-Tol (**2c**)	5.4	23.0
4	4-FC_6H_4 (**2d**)	2.6	23.5
5	*m*-Tol (**2e**)	3.1	23.4
6	3-(OMe)C_6H_4 (**2f**)	2.3	23.6
7[b]	3-FC_6H_4 (**2g**)	0.55	24.5
8[c]	2-(t-Bu)C_6H_4 (**2h**)	2.5 (65 °C)	25.5
9	4-F-2-(OMe)C_6H_3 (**2i**)	2.7	23.5

[a]Reactions performed as shown in Scheme 2; rate constants determined by fitting a plot of [**2**] vs time for 5 half-lives of data to the equation for an exponential decay; averages from two experiments; deviations were within 20% of the average value.

[b]Rate constant was determined from the linear fit of a ln[**2g**] vs time plot (1.3 half-lives).

[c]Reaction monitored at 338 K.

Table 3.

Effects of Substituents on the Ancillary Ligand on the Rate of Reductive Elimination[a]

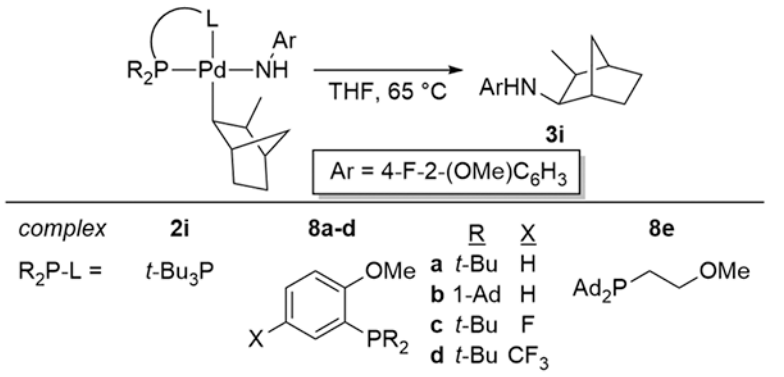

entry	complex	$k_{RE} \times 10^5$ (s^{-1})	$\Delta G_{RE}^{\ddagger}$ (kcal·mol $^{-1}$)
1[b]	**2i**	ca. 300	23.8
2[c]	**8a**	2.7	26.9
3	**8b**	2.9	26.9
4[d]	**8c**	25	25.4
5[e]	**8d**	14	25.8
6	**8e**	18	25.7

[a]Conditions: Pd-NHAr **8a–e** (0.020 mmol) and phosphine (3 equiv) in THF (0.70 mL) at 65 °C in a VT NMR probe; concentrations were determined by ^{19}F NMR spectroscopy with 4-FTol as internal standard; rate constants and activation energies were determined from linear fits of ln[**8**] vs time plots (1 half-life).

[b]The k_{RE} and $\Delta G_{RE}^{\ddagger}$ for **2i** at 65 °C were extrapolated from the data in Figure 2b.

[c]Data averaged from two experiments.

[d]Complex **8c** underwent significant (ca. 50%) unproductive decomposition during this experiment; the rate constant is approximate and an overestimation.

[e]Attempts to isolate and purify **8d** were unsuccessful; a solution of **8d** in THF was generated by the method described in Scheme 2 for this experiment.

Table 4.

Calculated Effects of Ancillary Ligands on Reductive Elimination To Form sp^3 C–N Bonds[a]

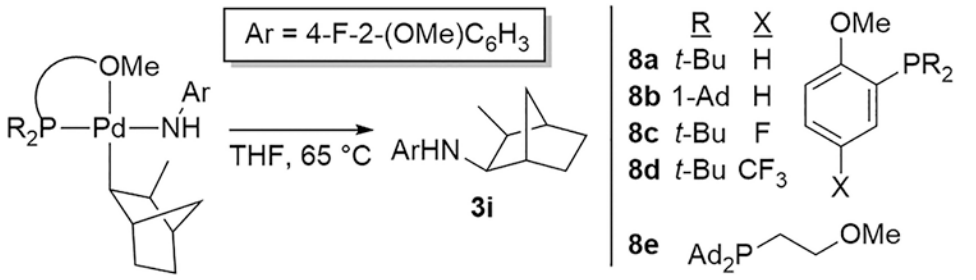

entry	complex	Pd−O (Å)	C−Pd−N (deg)	$\Delta G_{RE}^{\ddagger}$ (kcal·mol $^{-1}$)
1	**8a**	2.46 (2.89)	95.0 (56.9)	26.9
2	**8b**	2.45 (2.87)	94.7 (56.5)	25.8
3	**8c**	2.47 (2.90)	95.1 (57.2)	25.8
4	**8d**	2.48 (2.88)	95.4 (57.1)	25.5
5	**8e**	2.47 (3.87)	95.3 (58.6)	23.1

[a] Pd–O and C–Pd–N values are from ground state calculations. Values in parentheses are from the corresponding optimized transition state structures. Barriers are calculated with temperatures at 338 K.

Table 5.

Effects of Anilido Substituents on the Calculated Barrier to Reductive Elimination from 2a–i to form 3a–i[a]

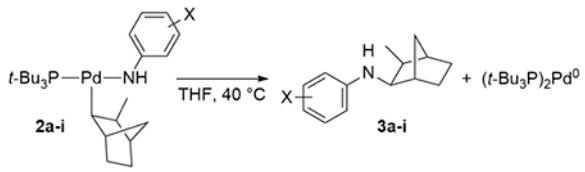

entry	X	ΔG_{RE}* (kcal·mol $^{-1}$)[a]
1	H (**2a**)	21.9
2	4-OMe (**2b**)	22.7
3	4-Me (**2c**)	22.8
4	4-F (**2d**)	23.4
5	3-Me (**2e**)	22.6 (1.0), 23.7
6	3-OMe (**2f**)	22.9, 23.4 (0.8)
7	3-F (**2g**)	24.3 (1.6), 24.7
8[b]	2-t-Bu (**2h**)	25.2, 32.8 (7.3)
9	2-OMe-4-F (**2i**)	23.4, 26.7 (4.2)

[a] $\Delta G^{\ddagger}$ values for both conformers by C–N rotation reported relative to the lower ground state (ΔG_{isom}, the relative energy of the isomeric ground state, reported in parentheses).

[b] Calculated temperatures at 338 K.